J. Fluid Mech. (1988), *vol.* 195, *pp.* 463–494
Printed in Great Britain

Nonlinear stability of evaporating/condensing liquid films

By J. P. BURELBACH†, S. G. BANKOFF† AND S. H. DAVIS‡

† Department of Chemical Engineering, The Technological Institute, Northwestern University, Evanston, IL 60208, USA

‡ Department of Engineering Sciences and Applied Mathematics, The Technological Institute, Northwestern University, Evanston, IL 60208, USA

(Received 17 October 1987 and in revised form 2 May 1988)

We consider horizontal static liquid layers on planar solid boundaries and analyse their instabilities. The layers are either evaporating, when the plates are heated, or condensing, when the plates are cooled. Vapour recoil, thermocapillary, and rupture instabilities are discussed, along with the effects of mass loss (or gain) and non-equilibrium thermodynamic effects. Particular attention is paid to the development of dryout. We derive long-wave evolution equations for the interface shapes that govern the two-dimensional nonlinear stability of the layers subject to the above coupled mechanisms. These equations are analysed and their predictions discussed. Previous theoretical and experimental results are reviewed and compared with the present results. Finally, we discuss limitations of the modelling and extend our derivation to the case of three-dimensional disturbances.

1. Introduction

A liquid layer lies on a planar, solid boundary. There is a mode of instability present when the layer is ultra-thin (100–1000 Å) which is driven, even in a static layer, by long-range molecular forces due to van der Waals attractions (Sheludko 1967) and results in the rupture of the layer. Such a film possesses a difference in chemical potential with respect to a large phase of the same material, resulting in a corresponding change in all intensive thermodynamic properties. Deryagin first recognized the thermodynamic significance of dimension; he terms as 'disjoining pressure' the excess pressure in a thin layer compared with that in a phase of infinite extent (Deryagin & Kusakov 1937; Deryagin 1955). A negative disjoining pressure is characteristic of a film having a higher pressure than the bulk phase, as when long-range molecular forces due to van der Waals attractions are considered. In that case spontaneous thinning occurs, and the film interfaces decrease in separation distance. When electric double-layer forces are considered, the added disjoining pressure component is positive and the competition between these and the van der Waals attractions can lead to the formation of black films (Overbeek 1960).

Lifshitz (1955) constructed a general macroscopic theory of the attractive van der Waals forces between bodies whose characteristic dimensions are large relative to interatomic distances. He found that the force of mutual attraction acting on unit surface of each of the bodies is inversely proportional to d^3 or d^4, when the separation distance d is small or large, respectively, compared with the wavelengths that are important in the absorption spectra of the bodies. Application of the methods of quantum field theory makes it possible to find the general formulae for the

calculation of the van der Waals part of the thermodynamic quantities for an arbitrary inhomogeneous medium (Dzyaloshinskii & Pitaevskii 1959). This allows the theory of Lifshitz to be extended to bodies separated by a liquid layer, and leads to its application to the study of liquid films (Dzyaloshinskii, Lifshitz & Pitaevskii 1959).

The problem of finding the thickness at which a non-thinning film becomes unstable owing to van der Waals forces was considered by Vrij (1966), who used a static stability analysis to calculate a marginally stable thickness at which small disturbances first start to grow. A dynamic linear stability theory for an isothermal film on a horizontal plate (Ruckenstein & Jain 1974), based on the Navier–Stokes equations modified with an extra body force due to van der Waals attractions, shows that an initial disturbance periodic along the bounding plane has a critical wavelength much larger than the mean depth of the layer. Gumerman & Homsy (1975) examined the linear stability of radially bounded thinning free films for which the base state is a time-dependent drainage flow computed by lubrication theory. Williams & Davis (1982) posed a nonlinear stability theory based on the long-wave nature of the response. They derived a partial differential equation which describes the evolution of the interface shape subject to surface tension, viscous forces, plus van der Waals attractions. Davis (1983) discussed the generalization of the result to a (non-volatile) film on a heated plate, accounting for thermocapillary and gravity-wave effects.

When the plate is heated, the latent heat required for evaporation is balanced by the heat flux across the liquid film, and large temperature differences may be maintained. This allows the rapid removal of heat from the hot surface. (Condensation involves a similar but oppositely directed transfer of latent heat.) New modes of instability develop at an evaporating liquid surface (Hickman 1952, 1972; Palmer & Maheshri 1981). Hickman noted that vapour recoil can induce hydrodynamic instability. Since a fluid particle conserves its mass flux upon phase change, a slowly moving liquid particle at the interface accelerates greatly when it becomes vapourized; the vapour particle has much lower density than does the liquid particle. The back reaction on the interface is called vapour recoil. A disturbance in the evaporating interface can result in a local increase in the evaporation rate at a surface depression or 'trough', producing a local increase in the normal force due to vapour recoil. The associated pressure gradient drives liquid towards the 'crests', amplifying the disturbance. In a similar manner, a disturbance in a condensing interface can result in a local increase in condensation. The condensing fluid particles likewise exert a destabilizing normal force.

An interpretation of instabilities associated with a moving boundary was given by Miller (1973), who examined the linear stability of an evaporating interface subject to the restriction that the interfacial temperature remains constant while the local rate of phase transformation is perturbed. Palmer (1976) expanded Miller's result to include the more realistic condition of a liquid whose evaporation rate depends on the interfacial temperature. If the depressed region experiences a local increase in surface temperature, then the induced gradient in surface tension induces a thermocapillary flow of warmer liquid from the trough to the cooler crests to amplify the disturbance; this is a mode of Marangoni instability (cf. Davis 1987). A more recent linear stability analysis for a rapidly evaporating liquid surface has been carried out by Prosperetti & Plesset (1984). They treat the liquid and vapour as inviscid fluids and obtain the perturbation growth rate as a function of the wavenumber. Higuera (1987)

generalized the analysis to include the effects of fluid viscosities when the vapour-to-liquid density ratio is small.

Bankoff (1971) studied the linear instability of an evaporating liquid film draining down an inclined heated plate. The film thickness is assumed to be so small that the Péclet number is small compared with unity, and the thermal time constant of the undisturbed film is small compared with either the convective time constant or the wave period. The evaporating interface is assumed to be always at the saturation temperature. Subsequent investigators (Marschall & Lee 1973; Unsal & Thomas 1978) removed the limitation of small Péclet numbers. They also included some additional effects, such as the liquid-momentum flux into the evaporating interface, that are omitted in the Bankoff analysis and which turn out to be small unless the pressure is very high. Spindler, Solesio & Delhaye (1978) pointed out and rectified deficiencies in the balance equations used by Bankoff (1971) and Marschall & Lee (1973). Spindler (1982) later reconsidered the full linear stability problem, taking into account the development in the mean thickness of the film due to evaporation as it drains down the wall, and also including the induced vapour shear stress. The numerical results obtained are similar to those obtained previously.

Clearly, the breakdown of a liquid layer into one with dry regions can occur in complex systems in which the rupture instability interacts with other instabilities. In fact, if one has a relatively thick film, one instability can create locally thin areas in the layer in which the van der Waals attractions can become effective in driving the layer to rupture. Thus, there can be a two-stage process, viz. a dynamical thinning followed by a rupture instability. We pursue this line of inquiry here for a static horizontal layer heated from below. The film is assumed to be initially thick (say, 0.1 mm thick), but it evaporates until it is much thinner (say, 0.1 μm thick). After the thinning of the film due to evaporation, there follows further non-uniform thinning due to the disjoining pressures induced by van der Waals attractions, which can cause rapid rupture of the very thin film. In this later stage, disjoining pressures can cause local rupture, or evaporative effects can cause dryout due to mass loss or vapour-recoil instabilities. We examine these conditions by extending the nonlinear theory developed by Williams & Davis (1982) to include evaporative, thermocapillary, and non-equilibrium effects, in addition to disjoining pressures induced by van der Waals attractions. Effects of condensation are similarly considered.

2. Formulation – one-sided model

We consider a thin viscous liquid layer bounded above by its vapour and below by a uniformly heated rigid plane. The layer is thin enough that gravity effects are negligible and van der Waals attractions are effective, but thick enough that a continuum theory of the liquid is applicable. The film is non-draining and laterally unbounded, and consists of an incompressible Newtonian fluid with constant material properties. The layer is evaporating, so that at the vapour–liquid interface there is mass loss, momentum transfer, and energy consumption.

The configuration is shown in figure 1, where Cartesian coordinates are used to describe the system, taken for convenience to be two-dimensional. The vapour–liquid interface is located at $z = h(x,t)$, where z is the vertical coordinate, and the film thickness h is a function of the lateral coordinate x and time t. The solid plate is located at $z = 0$. $J(x,t)$ is the mass flux due to evaporation, $T^{(I)}(x,t)$ is the temperature of the interface, and T_H is the (constant) temperature of the heated

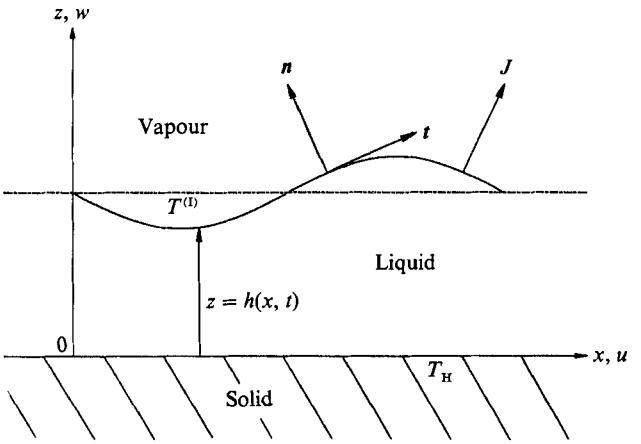

FIGURE 1. The physical configuration describing an evaporating thin liquid film on a horizontal heated solid surface.

plate. The unit vectors $\boldsymbol{n}$ and $\boldsymbol{t}$ are the outward normal and tangent vectors, respectively:

$$\boldsymbol{n} = (-h_x, 1)(1+h_x^2)^{-\frac{1}{2}}, \quad \boldsymbol{t} = (1, h_x)(1+h_x^2)^{-\frac{1}{2}}. \tag{2.1a,b}$$

Liquid is assumed to evaporate in a direction normal to the interface.

The liquid is taken to be a charge-neutral dielectric, such that electrical double-layer forces are negligible. The van der Waals forces are represented through the potential function ϕ which depends on the layer thickness:

$$\phi = \phi(h). \tag{2.2}$$

We follow Ruckenstein & Jain (1974) and augment the Navier–Stokes equations for the liquid with an extra body force, $\nabla\phi$, that models the van der Waals attractions:

$$\rho(\boldsymbol{v}_t + \boldsymbol{v}\cdot\nabla\boldsymbol{v}) = -\nabla p - \nabla\phi + \mu\nabla^2\boldsymbol{v}, \tag{2.3}$$

where ρ is the liquid density and μ is the dynamic viscosity. Here p denotes the pressure in the liquid, and $\boldsymbol{v}$ is the liquid velocity vector with components u and w in the x- and z-directions, respectively. Unless otherwise indicated, all quantities mentioned hereafter refer to the liquid phase.

The continuity and energy equations in the liquid are

$$\nabla\cdot\boldsymbol{v} = 0, \tag{2.4}$$

and

$$T_t + \boldsymbol{v}\cdot\nabla T = \kappa\nabla^2 T, \tag{2.5}$$

respectively, where κ is the thermal diffusivity and T is the temperature. The Navier-Stokes, continuity, and energy equations for the vapour are similar to (2.3)–(2.5), but with suitable modification and neglect of van der Waals forces.

At the heated solid boundary, $z = 0$, we assume no slip:

$$\boldsymbol{v} = \boldsymbol{0}, \tag{2.6}$$

and a constant temperature:

$$T = T_H. \tag{2.7}$$

At the interface, $z = h(x,t)$, there are the vapour–liquid jump conditions (cf. Delhaye 1974). The jump mass balance is

$$J = \rho(\boldsymbol{v}-\boldsymbol{v}^{(I)})\cdot\boldsymbol{n} = \rho^{(V)}(\boldsymbol{v}^{(V)}-\boldsymbol{v}^{(I)})\cdot\boldsymbol{n}, \tag{2.8a,b}$$

where $\boldsymbol{v}^{(\mathrm{V})}$ is the vapour velocity, $\boldsymbol{v}^{(\mathrm{I})}$ is the velocity of the interface, and the vapour density $\rho^{(\mathrm{V})}$ is assumed constant. There is also the jump energy balance:

$$J\{L+\tfrac{1}{2}[(\boldsymbol{v}^{\mathrm{V}})-\boldsymbol{v}^{(\mathrm{I})})\cdot\boldsymbol{n}]^2-\tfrac{1}{2}[(\boldsymbol{v}-\boldsymbol{v}^{(\mathrm{I})})\cdot\boldsymbol{n}]^2\}+k\nabla T\cdot\boldsymbol{n}-k^{(\mathrm{V})}VT''''\cdot\boldsymbol{n}$$
$$+2\mu(\boldsymbol{\tau}\cdot\boldsymbol{n})\cdot(\boldsymbol{v}-\boldsymbol{v}^{(\mathrm{I})})-2\mu^{(\mathrm{V})}(\boldsymbol{\tau}^{(\mathrm{V})}\cdot\boldsymbol{n})\cdot(\boldsymbol{v}^{(\mathrm{V})}-\boldsymbol{v}^{(\mathrm{I})})=0, \quad (2.9)$$

where $\boldsymbol{\tau}$ and $\boldsymbol{\tau}^{(\mathrm{V})}$ are the rate-of-deformation tensors in the liquid and vapour, respectively, L is the latent heat of vaporization, $T^{(\mathrm{V})}$ is the vapour temperature, and k and $k^{(\mathrm{V})}$ are the thermal eonductivities of the liquid and vapour, respectively. The normal-stress boundary condition,

$$J(\boldsymbol{v}-\boldsymbol{v}^{(\mathrm{V})})\cdot\boldsymbol{n}-(\boldsymbol{T}-\boldsymbol{T}^{(\mathrm{V})})\cdot\boldsymbol{n}\cdot\boldsymbol{n}=2H\sigma(T), \quad (2.10)$$

balances the jump in normal stress with surface tension σ times twice the mean curvature H of the interface,

$$2H=\nabla\cdot\boldsymbol{n}. \quad (2.11)$$

Here $\boldsymbol{T}$ and $\boldsymbol{T}^{(\mathrm{V})}$ are the stress tensors of the liquid and vapour, respectively. The shear-stress boundary condition,

$$J(\boldsymbol{v}-\boldsymbol{v}^{(\mathrm{V})})\cdot\boldsymbol{t}-(\boldsymbol{T}-\boldsymbol{T}^{(\mathrm{V})})\cdot\boldsymbol{n}\cdot\boldsymbol{t}=-\nabla\sigma\cdot\boldsymbol{t}, \quad (2.12)$$

balances the jump in shear stress with the surface-tension gradient.

Surface tension is represented by a linear equation of state,

$$\sigma=\sigma_0-\gamma(T^{(\mathrm{I})}-T_{\mathrm{S}}), \quad (2.13)$$

where σ_0 is the surface tension at the reference temperature T_{S}, taken as the saturation temperature at the system pressure. For nearly all common liquids $\gamma=-\mathrm{d}\sigma/\mathrm{d}T$ is positive. We assume no slip at the interface between the two viscous fluids:

$$(v-\boldsymbol{v}^{(\mathrm{V})})\cdot\boldsymbol{t}=0. \quad (2.14)$$

The linearized constitutive equation,

$$J=\left(\frac{\alpha\rho^{(\mathrm{V})}L}{T_{\mathrm{S}}^{\frac{3}{2}}}\right)\left(\frac{M_{\mathrm{W}}}{2\pi R_{\mathrm{g}}}\right)^{\frac{1}{2}}(T^{(\mathrm{I})}-T_{\mathrm{S}}), \quad (2.15)$$

is derived from kinetic theory (cf. Palmer 1976). It relates the mass flux J at the interface to the local surface temperature $T^{(\mathrm{I})}$, where M_{W} is the molecular weight, R_{g} is the universal gas constant, and α is the accommodation coefficient.

Finally, appropriate initial conditions must also be specified for the film thickness and the velocity and temperature fields.

Having formulated the two-fluid problem (without boundary conditions at the top of the vapour layer), we consider a limiting case and assume that density, viscosity, and thermal conductivity are all much greater in the liquid than in the vapour. Formally, we take the limits

$$\frac{\rho^{(\mathrm{V})}}{P}\to 0, \quad \frac{\mu^{(\mathrm{V})}}{\mu}\to 0, \quad \frac{k^{(\mathrm{V})}}{\mathrm{k}}\to 0. \quad (2.16\text{a-c})$$

However, we retain the vapour density in (2.8*b*) where it multiplies the vapour velocity, which may be large. (This is similar in spirit to the Boussinesq approximation of thermal convection, in which density variations are neglected except in association with gravity.) However, we assume that the vapour velocity is sufficiently slow (small Mach number) that the vapour and liquid may both be

treated as incompressible Newtonian fluids. The stress tensor in the liquid is written as

$$\boldsymbol{T} = -p\boldsymbol{I} + 2\mu\boldsymbol{\tau}, \tag{2.17}$$

where $\boldsymbol{I}$ is the identity tensor; a similar form is used for the vapour stress tensor. Finally, we take the pressure in the gas, $p^{(V)}$, to be zero.

The jump conditions at the vapour–liquid interface are simplified as follows. In the jump energy balance (2.9) we express velocities in terms of the mass flux and density by substituting from the jump mass balance (2.8*a*, *b*). We assume $\nabla T^{(V)} \cdot \boldsymbol{n}$, $\boldsymbol{\tau} \cdot \boldsymbol{n} \cdot \boldsymbol{n}$, and $\boldsymbol{\tau}^{(V)} \cdot \boldsymbol{n} \cdot \boldsymbol{n}$ are all bounded and apply the limits (2.16) to get

$$J\left\{L + \frac{1}{2}\left[\frac{J}{\rho^{(V)}}\right]^2\right\} = -k\nabla T \cdot \boldsymbol{n}, \tag{2.18}$$

which states that the heat conducted across the film is used to vaporize liquid and impart kinetic energy to the vapour particles. In the normal-stress balance (2.10) we again substitute for velocities from the jump mass balance and apply the limits (2.16*a*, *b*) to get

$$-\frac{J^2}{\rho^{(V)}} - \boldsymbol{T} \cdot \boldsymbol{n} \cdot \boldsymbol{n} = 2H\sigma(T), \tag{2.19}$$

where the term proportional to J^2 results from vapour recoil. In the shear-stress balance we use the no-slip condition (2.14) to eliminate the first term on the left-hand side of (2.12). Substituting for the stress tensors as before and applying the limit (2.16*b*), we get simply

$$\boldsymbol{T} \cdot \boldsymbol{n} \cdot \boldsymbol{t} = \nabla\sigma \cdot \boldsymbol{t}. \tag{2.20}$$

The remaining jump conditions, (2.8) and (2.15), remain unchanged, as do the boundary conditions at the solid plate.

The dynamics of the vapour are thus decoupled from the dynamics of the liquid, yielding what we call the *one-sided model* of evaporation. This one-sided model extends that posed by Spindler et *al.* (1978) for a falling film to include non-equilibrium effects, van der Waals attractions, vapour kinetic energy and a full set of boundary conditions. This is the starting point for our analysis.

3. Scaling of the one-sided model

We now non-dimensionalize the governing equations and boundary conditions. Length is scaled on the mean film thickness d_0 at the initial time $t = 0$. Viscous scales are chosen for time, velocity, and pressure. These are, respectively, d_0^2/ν, ν/d_0, and $\rho\nu^2/d_0^2$, where ν is the kinematic viscosity of the liquid. These scales are appropriate to an isothermal layer in which surface tension, viscosity, and van der Waals attractions influence film rupture (cf. Williams & Davis 1982). They should also apply when the layer is non-isothermal and the evaporation is not too intense. The saturation temperature T_S is again taken as a reference, and the temperature difference $T - T_S$ is scaled on the temperature difference $\Delta T = T_H - T_S$. Mass flux is scaled on its initial value for a linear temperature profile across an initially flat film, viz. $k\,\Delta T/d_0\,L$. In addition to the viscous timescale, there is also an evaporative timescale : $t_E = \rho d_0^2\,L/k\,\Delta T$. Although this evaporative scale is not employed in the initial scaling, it does appear in the scaled equations through a parameter E, which is the ratio of the viscous to evaporative timescales. Since the viscous timescale $t_V = d_0^2/\nu$ is assumed to be much shorter than the evaporative scale, this ratio is small.

The Navier–Stokes and continuity equations are

$$\boldsymbol{v}_t + \boldsymbol{v}\cdot\boldsymbol{\nabla}\boldsymbol{v} = -\boldsymbol{\nabla}p - \boldsymbol{\nabla}\phi + \nabla^2\boldsymbol{v} \tag{3.1}$$

and

$$\boldsymbol{\nabla}\cdot\boldsymbol{v} = 0. \tag{3.2}$$

We follow Ruckenstein & Jain (1974) and write the potential function ϕ as

$$\phi = Ah^{-3}, \tag{3.3a}$$

where the exponent is chosen for convenience and the dimensional Hamaker constant A' is related to A by

$$A = \frac{A'}{6\pi d_0 \rho\nu^2}. \tag{3.3b}$$

Note that this potential for the van der Waals attractions is independent of z. We consider here the case $A' > 0$, usually called the case of negative disjoining pressure, which corresponds to a destabilizing van der Waals force. The scaled energy equation is

$$P(T_t + \boldsymbol{v}\cdot\boldsymbol{\nabla}T) = \nabla^2 T, \tag{3.4}$$

where P is the Prandtl number

$$P = \nu/\kappa. \tag{3.5}$$

At the heated solid surface, $z = 0$, the boundary conditions are

$$\boldsymbol{v} = \boldsymbol{0}, \quad T = 1. \tag{3.6a,b}$$

At the interface, $z = h(x,t)$, the scaled jump mass balance is

$$EJ = (\boldsymbol{v} - \boldsymbol{v}^{(\mathrm{I})})\cdot\boldsymbol{n} = \tfrac{2}{3}D(\boldsymbol{v}^{(\mathrm{V})} - \boldsymbol{v}^{(\mathrm{I})})\cdot\boldsymbol{n}. \tag{3.7a,b}$$

We term the ratio of the viscous to evaporative timescales the 'evaporation number',

$$E = \frac{k\Delta T}{\rho\nu L}. \tag{3.8}$$

For slow evaporation E is small. The parameter D is proportional to the ratio of the vapour to liquid densities,

$$D = \frac{3}{2}\frac{\rho^{(\mathrm{V})}}{\rho}. \tag{3.9}$$

In most cases D is very small. The scaled energy jump is

$$J + (E^2 D^{-2}\mathscr{L}^{-1})J^3 = -\boldsymbol{\nabla}T\cdot\boldsymbol{n}, \tag{3.10}$$

where

$$\mathscr{L} = \frac{8}{9}\frac{d_0^2 L}{\nu^2} \tag{3.11}$$

is a measure of the latent heat. The scaled normal-stress condition is

$$-\tfrac{3}{2}E^2 D^{-1}J^2 + p - 2\boldsymbol{\tau}\cdot\boldsymbol{n}\cdot\boldsymbol{n} = 3S(1 - CT)\,\boldsymbol{\nabla}\cdot\boldsymbol{n}. \tag{3.12}$$

The non-dimensional surface tension S is defined as

$$S = \frac{\sigma_0 d_0}{3\rho\nu^2}, \tag{3.13}$$

while the capillary number C is given by

$$C = \frac{\gamma\Delta T}{\sigma_0}. \tag{3.14}$$

The scaled shear-stress condition is

$$\boldsymbol{\tau}\cdot\boldsymbol{n}\cdot\boldsymbol{t} = -MP^{-1}\nabla T\cdot\boldsymbol{t}, \tag{3.15}$$

were M is the Marangoni number,

$$M = \frac{\gamma\,\Delta T d_0}{2\rho\nu\kappa}. \tag{3.16}$$

We also have the scaled constitutive equation,

$$KJ = T, \tag{3.17}$$

where

$$K = \left(\frac{kT_S^{\frac{3}{2}}}{\alpha d_0 \rho^{(V)} I^2}\right)\left(\frac{2\pi R_g}{M_W}\right)^{\frac{1}{2}}. \tag{3.18}$$

The parameter K measures the degree of non-equilibrium at the evaporating interface. $K = 0$ corresponds to the quasi-equilibrium limit, where the interfacial temperature is constant and equal to the saturation value, $T = 0$. $K^{-1} = 0$ corresponds to the non-volatile case in which the evaporative mass flux J is zero.

In component form, the scaled governing system is as follows. The x- and z-components of the Navier–Stokes equation are, respectively,

$$u_t + uu_x + wu_z = -(p_x + \phi_x) + u_{xx} + u_{zz} \tag{3.19}$$

and

$$w_t + uw_x + ww_z = -p_z + w_{xx} + w_{zz}. \tag{3.20}$$

The continuity equation is

$$u_x + w_z = 0, \tag{3.21}$$

and the energy equation is

$$P(T_t + uT_x + wT_z) = T_{xx} + T_{zz}. \tag{3.22}$$

The boundary conditions at the solid surface ($z = 0$) are

$$u = 0, \quad w = 0, \quad T = 1. \tag{3.23a–c}$$

At the interface ($z = h$) we have, from the jump mass balance,

$$EJ = (-h_t - uh_x + w)(1 + h_x^2)^{-\frac{1}{2}}, \tag{3.24}$$

which is the kinematic boundary condition for an interface that is not a material surface. The energy balance is

$$J + (E^2 D^{-2}\mathscr{L}^{-1})J^3 = (T_x h_x - T_z)(1 + h_x^2)^{-\frac{1}{2}}. \tag{3.25}$$

The normal-stress condition is

$$-\tfrac{3}{2}E^2 D^{-1}J^2 + p - 2[u_x(h_x^2 - 1) - h_x(u_z + w_x)](1 + h_x^2)^{-1} = -3S(1 - CT)\,h_{xx}(1 + h_x^2)^{-\frac{3}{2}}, \tag{3.26}$$

and the shear-stress condition is

$$(u_z + w_x)(1 - h_x^2) - 4u_x h_x = -2MP^{-1}(T_x + T_z h_x)(1 + h_x^2)^{\frac{1}{2}}. \tag{3.27}$$

The constitutive equation remains

$$KJ = T. \tag{3.28}$$

As a result of the scaling, several non-dimensional groups appear in the problem. Typical numerical values and the material properties from which they are computed are presented in table 1 for water and ethanol.

	Water	Ethanol
P (MPa)	0.101	0.101
T_s (K)	373	352
d_0 (cm)	10^{-6}	10^{-6}
ΔT (°C)	10	10
ρ (g/cm^3)	0.96	0.79
$\rho^{(V)}$ (g/cm^3)	0.6×10^{-3}	1.6×10^{-3}
ν (cm^2/s)	3.0×10^{-3}	5×10^{-3}
$\nu^{(V)}$ (cm^2/s)	0.21	0.62
k (erg/cm s °C)	6.8×10^{4}	1.7×10^{4}
$k^{(V)}$ (erg/cm s °C)	2.4×10^{3}	1.7×10^{3}
κ (cm^2/s)	1.7×10^{-3}	8.8×10^{-4}
$\kappa^{(V)}$ (cm^2/s)	0.2	0.07
L (J/g)	2.3×10^{3}	8.8×10^{2}
M_w (g/gmole)	18	46
σ_0 (dynes/cm)	59	20
γ (dynes/cm °C)	0.18	0.9
A' (erg)	10^{-13}	10^{-13}
A	10^{-3}	10^{-4}
C	10^{-2}	10^{-1}
D	10^{-3}	10^{-3}
E	10^{-2}	10^{-3}
K	10	1
$\mathscr{L}$	10^{3}	10^{2}
M	10^{-1}	1
P	1	10
S	1	10^{-1}
$\mathscr{E}$	10^{4}	10^{4}
$\mathscr{D}$	10^{5}	10^{4}
$\mathscr{M}$	10^{5}	10^{6}
G	10^{-11}	10^{-11}

TABLE 1. Material properties and dimensionless groups for liquids at 1 atm. In each case the film is 100 Å thick and the plate temperature is 10 °C above the saturation temperature T_s.

4. Basic state

Since the heated film is evaporating, the basic state is time-dependent; we denote basic state quantities by an overbar. The basic state is assumed to be static with a flat evaporating interface. Thus there is no dependence on the lateral coordinate x, and the basic-state velocity field is zero. The Navier–Stokes equation (3.20) is simply

$$\bar{p}_z = 0, \tag{4.1}$$

while the energy equation (3.22) is

$$P\bar{T}_t = \bar{T}_{zz}. \tag{4.2}$$

At the solid boundary, $z = 0$, condition (3.23c) remains

$$\bar{T} = 1. \tag{4.3}$$

At the interface, $z = \bar{h}(t)$, the kinematic boundary condition (3.24) becomes

$$E\bar{J} = -\bar{h}_t, \tag{4.4}$$

while the energy jump (3.25) is

$$\bar{J} + (E^2D^{-2}\mathscr{L}^{-1})\bar{J}^3 = -\bar{T}_z. \tag{4.5}$$

The jump in normal stress (3.26) is

$$-\tfrac{3}{2}E^2D^{-1}\bar{J}^2+\bar{p}=0, \tag{4.6}$$

and there is no shear stress in the basic state. The constitutive equation (3.28) remains

$$K\bar{J}=\bar{T}. \tag{4.7}$$

To retain the effect of mass loss in the kinematic condition (4.4), we rescale time on the evaporative scale:

$$t'=Et, \quad z'=z. \tag{4.8a,b}$$

The mass flux $\bar{J}(t')$ and liquid temperature $\bar{T}(z',t')$ are assumed to be of order unity, but we take pressure $\bar{p}(t')$ to be of order E^{-1}. These dependent variables are expanded in powers of E:

$$\bar{J}=J_0+EJ_1+E^2J_2+\ldots, \tag{4.9a}$$

$$\bar{T}=T_0+ET_1+E^2T_2+\ldots, \tag{4.9b}$$

$$\bar{p}=E^{-1}(p_0+Ep_1+\ldots), \tag{4.9c}$$

while the film thickness $\bar{h}(t')$ is considered an unspecified order-one function. In order to retain vapour recoil in the normal-stress balance, the relationship between the small parameters D and E is assumed to be of the form

$$D=\bar{D}E^3, \tag{4.10}$$

where $\bar{D}$ is an order-one quantity. Table 1 indicates that the parameter $\mathscr{L}$ is typically quite large. We therefore assume

$$\mathscr{L}^{-1}=o(1) \tag{4.11}$$

so that the kinetic energy in the jump energy balance is neglected.

After applying the transformation (4.8) and substituting expansions (4.9) into (4.1)–(4.7), the leading-order system governing the basic state becomes

$$p_{0_{z'}}=0, \tag{4.12}$$

$$T_{0_{z'z'}}=0, \tag{4.13}$$

$z'=0$

$$T_0=1, \tag{4.14}$$

$z'=\bar{h}(t')$:

$$\begin{cases} J_0=-\bar{h}_{t'}, & (4.15a)\\ J_0=-T_{0_{z'}}, & (4.15b)\\ E^{-1}p_0=\tfrac{3}{2}E^2D^{-1}J_0^2, & (4.15c)\\ KJ_0=T_0, & (4.15d) \end{cases}$$

along with the initial condition

$$t'=0: \quad \bar{h}=1. \tag{4.16}$$

Note that, in this small-E limit, (4.13) describes a quasi-steady temperature field. The resulting leading-order basic-state solution is

$$\bar{h}=-K+(K^2+2K+1-2Et)^{\frac{1}{2}}, \tag{4.17a}$$

$$\bar{T}=1-(K^2+2K+1-2Et)^{-\frac{1}{2}}z, \tag{4.17b}$$

$$\bar{J}=(K^2+2K+1-2Et)^{-\frac{1}{2}}, \tag{4.17c}$$

$$\bar{p}=\tfrac{3}{2}E^2D^{-1}(K^2+2K+1-2Et)^{-1}. \tag{4.17d}$$

Figure 2 details the behaviour of this solution for quasi-equilibrium ($K=0$), non-equilibrium ($K\neq 0$) and non-volatile ($K^{-1}=0$) cases.

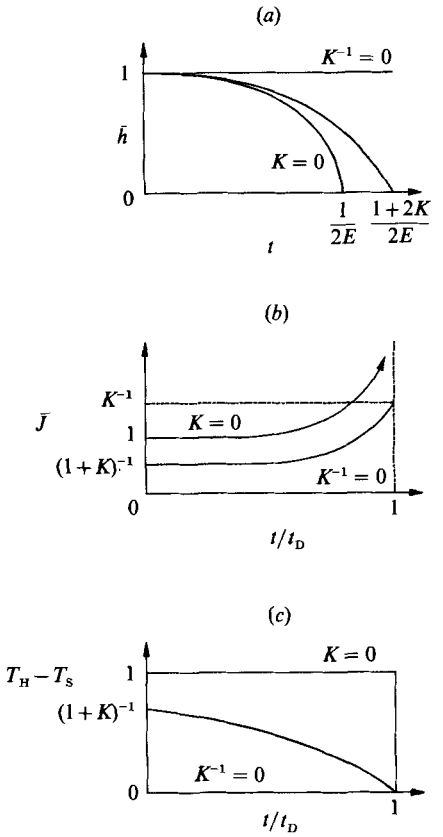

FIGURE 2. Basic-state behaviour for various degrees of non-equilibrium evaporation.

4.1. *Quasi-equilibrium case* ($K = 0$)

According to (4.17a), when $K = 0$ the film thickness $\bar{h} \approx (1-2Et)^{\frac{1}{2}}$ goes to zero with velocity $\bar{h}_t \to -\infty$ at the disappearance time $t_D = 1/2E$ (figure 2a). The evaporative mass flux $\bar{J} \approx (1-2Et)^{-\frac{1}{2}}$ is initially unity but becomes unbounded at $t = t_D$ (figure 2b), since the temperature difference across the vanishing film is a fixed constant (figure 2c). Thus, singularities occur in (4.17), since $\bar{J} \to \infty$ as $t \to t_D$ and $\bar{p}$ depends directly on the vapour recoil. The solution (4.17) breaks down near disappearance because the higher-order terms of (4.9) become comparable with those of leading order.

The basic-state temperature profile does not satisfy the arbitrary initial temperature condition $T(z,0) = \theta_0(z)$, since, in the formal limit $E \to 0$, the temperature field satisfies the quasi-steady conduction equation (4.13).

The non-uniformities at early and late times can be analysed by the introduction of boundary layers in $O(E)$ neighbourhoods near $t = 0$ and $t = t_D$. Multiple scales and matched asymptotics may then be used to find the inner solutions. Details are given by Burelbach (1989). We find that the initial temperature field adjusts in a time of $O(E)$ to the linear (quasi-steady) profile, and negligible evaporation occurs during this adjustment period. A late-time analysis yields a solution that breaks down at higher order. However, since we expect disturbances to grow or decay much faster than the basic-state film thickness goes to zero, this late-time limitation does not seriously affect our analysis. In any case, at late times the lubrication approximation

that we employ is not valid since the film thickness does not vary slowly with time.

4.2. *Non-equilibrium case* ($K \neq 0$)

When $K \neq 0$ and finite, the film approaches zero thickness with finite velocity at the time $t_D = (1+2K)/2E$ (figure 2*a*). The mass flux is initially $(1+K)^{-1}$ but increases to K^{-1} at the disappearance time (figure 2*b*). The temperature difference across the thinning film is initially $(1+K)^{-1}$ but decreases to zero as the film disappears and the interface temperature T_S approaches the wall temperature T_H (figure 2*c*). Singularities again occur in (4.17), at time $t = (1+K)^2/2E$, but by then the film has already disappeared. Once again the satisfaction of arbitrary initial temperature data requires rescaling near $t = 0$.

4.3. *Non-volatile case* ($K^{-1} = 0$)

When $K^{-1} = 0$, no evaporation occurs (figure 2*b*) since there is a zero temperature gradient across the film (figure 2*c*), and the film thickness remains at unity (figure 2*a*).

5. Long-wave theory

The dynamic linear stability analysis of Ruckenstein & Jain (1974) shows for the *isothermal* problem that the initial instability, periodic along the bounding plane, has a critical wavelength much larger than the mean thickness of the liquid layer. Williams & Davis (1982) describe the interfacial deflection of this instability by a nonlinear stability theory based on the long-wave nature of the response. This method is related to those used by Benney (1966) and Atherton & Homsy (1976) for isothermal falling films in the absence of long-range forces.

We now consider the non-isothermal, evaporating layer and assume that the dependent variables vary slowly along the plate and in time so that lubrication theory may be used. Such an approximation excludes those small time intervals near $t = t_D$ and $t = 0$ where the basic state may be non-uniform in time; inside these regions the temperature profile or the film thickness change rapidly. We consider long-wave disturbances periodic in x and define as a small parameter the wavenumber k. We rescale the governing system consistent with lubrication theory by writing

$$\xi = kx, \quad \zeta = z, \quad \tau = kt. \tag{5.1}$$

We assume that $u, J, T = O(1)$ but require that $w = O(k)$ as $k \to 0$ to preserve continuity; to examine spontaneous rupture we take both $p, \phi = O(k^{-1})$ as $k \to 0$. These dependent variables are expanded in powers of k:

$$u = u_0 + ku_1 + \ldots, \quad w = k(w_0 + kw_1 + \ldots), \tag{5.2a,b}$$

$$J = J_0 + kJ_1 + \ldots, \quad T = T_0 + kT_1 + \ldots, \tag{5.2c,d}$$

$$p = k^{-1}(p_0 + kp_1 + \ldots), \quad \phi = k^{-1}\phi_0, \tag{5.2e,f}$$

while the film thickness $h(\xi, \tau)$ is considered an unspecified unit-order function. We proceed with the asymptotic analysis by substituting expansions (5.2) into the governing system. We equate to zero the coefficients of like powers of k in each equation and boundary condition and obtain a sequence of problems. We then determine the mass flux and velocity field as functions of film thickness. These solutions are substituted into the jump mass balance (i.e. the kinematic boundary condition) to obtain an equation describing the evolution of the interface.

Table 1 indicates that the parameter $\mathscr{L}$ is typically much larger than the quantity E^2D^{-2}, so that kinetic energy is neglected in this analysis. To include all the remaining physical effects that appear in the one-sided model we assume that A, D, E, M and S are related to k as follows:

$$(A, D, E, M, S) = (\bar{A}k^{-1}, \bar{D}k^3, \bar{E}k, \bar{M}k^{-1}, \bar{S}k^{-3}) \tag{5.3}$$

where quantities with overbars are $O(1)$ as $k \to 0$. To examine spontaneous rupture we follow Williams & Davis (1982) and take $A = O(k^{-1})$. We let $E = O(k)$ to include mass loss and $D = O(k^3)$ to retain vapour recoil. These last two assumptions allow us to formally neglect kinetic energy by assuming

$$\mathscr{L}^{-1} = o(k^4). \tag{5.4}$$

We assume $M = O(k^{-1})$ to retain the thermocapillary effect in the shear-stress condition and $S = O(k^{-3})$ to retain the effect of surface tension in the normal-stress condition. Note, however, that $\bar{S}C = \frac{2}{3}k^2\bar{M}P^{-1}$, so that when the shear stress is balanced by the surface-tension gradient, thermocapillary effects do not appear at leading order in the normal-stress balance. Finally, we require both $K, P = O(1)$.

At leading order in k, the governing system is

$$-p_{0_\xi} - \phi_{0_\xi} + u_{0_{\zeta\zeta}} = 0, \tag{5.5}$$

$$-p_{0_\zeta} = 0, \tag{5.6}$$

$$u_{0_\xi} + w_{0_\zeta} = 0, \tag{5.7}$$

$$T_{0_{\zeta\zeta}} = 0; \tag{5.8}$$

$\zeta = 0$:

$$u_0 = 0, \quad w_0 = 0, \quad T_0 = 1; \tag{5.9a–c}$$

$\zeta = h(\xi, \tau)$:

$$\bar{E}J_0 = w_0 - u_0 h_\xi - h_\tau, \tag{5.10a}$$

$$J_0 = -T_{0_\zeta}, \tag{5.10b}$$

$$p_0 = \tfrac{3}{2}\bar{E}^2\bar{D}^{-1}J_0^2 - 3\bar{S}h_{\xi\xi}, \tag{5.10c}$$

$$u_{0_\zeta} = -2\bar{M}P^{-1}(T_{0_\xi} + T_{0_\zeta}h_\xi), \tag{5.10d}$$

$$KJ_0 = T_0. \tag{5.10e}$$

Equations (5.5)–(5.10) yield a long-wave evolution equation which governs the nonlinear stability of the liquid layer subject to thermocapillary, evaporative, and rupture instabilities. We first solve (5.8) subject to conditions (5.9*c*), (5.10*b*) and (5.10*e*) to find the liquid temperature field,

$$T_0 = 1 - (h+K)^{-1}\zeta, \tag{5.11}$$

and the evaporative mass flux,

$$J_0 = (h+K)^{-1}. \tag{5.12}$$

Equation (5.12) is substituted into (5.10*c*); we solve (5.6), subject to condition (5.10*c*), to find the pressure in the liquid,

$$p_0 = \tfrac{3}{2}\bar{E}^2\bar{D}^{-1}(h+K)^{-2} - 3\bar{S}h_{\xi\xi}. \tag{5.13}$$

From (3.3*a*) we have

$$\phi_0 = \bar{A}h^{-3}. \tag{5.14}$$

Equations (5.13) and (5.14) are substituted into (5.5); we solve (5.5), subject to conditions (5.9*a*) and (5.10*d*), to find the x-component of the liquid velocity,

$$u_0 = \Phi[\tfrac{1}{2}\zeta^2 - h\zeta] + 2\bar{M}P^{-1}[h(h+K)^{-1}]_\xi\zeta, \tag{5.15}$$

where $$\Phi(\xi,\tau) = -3\bar{E}^2\bar{D}^{-1}(h+K)^{-3}h_\xi - 3\bar{S}h_{\xi\xi\xi} - 3\bar{A}h^{-4}h_\xi. \tag{5.16}$$

Equation (5.15) is substituted into (5.7), which we then solve, subject to condition (5.9*b*), to find the z-component of the liquid velocity,

$$w_0 = -\Phi_\xi[\tfrac{1}{6}\zeta^3 - \tfrac{1}{2}h\zeta^2] + \tfrac{1}{2}\Phi h_\xi\,\zeta^2 - \bar{M}P^{-1}[h(h+K)^{-1}]_{\xi\xi}\,\zeta^2. \tag{5.17}$$

Finally, we substitute (5.15)–(5.17) and (5.12) into (5.10*a*) and apply assumption (5.3) to obtain the result

$$h_t + E(h+K)^{-1} + S(h^3h_{xxx})_x + \{[Ah^{-1} + E^2D^{-1}(h+K)^{-3}h^3 + KMP^{-1}(h+K)^{-2}h^2]\,h_x\}_x = 0, \tag{5.18}$$

expressed in terms of the (unscaled) physical variables x and t. Notice that if we choose the exponent in (5.14) to be -4 rather than -3, then the van der Waals term becomes Ah^{-2}. Equation (5.18) represents a major step in the description of evaporating films. Rather than having to solve the free-boundary problem described in §2, we need only solve the single partial differential equation (5.18), subject to initial conditions.

6. Numerical method

Equation (5.18) is a strongly nonlinear partial differential equation. It is solved numerically in conservative form as part of an initial-value problem for spatially periodic solutions on the fixed interval $0 < x < 2\pi/k$. Centred differences in space are employed while the midpoint (Crank–Nicholson) rule is used in time. The difference equations are solved by Newton–Raphson iteration.

The mesh size is taken sufficiently small so that space and time errors are negligible (cf. Burelbach 1989). This is accomplished by first fixing the spatial grid while reducing the time step for successive computer runs until the change in the computed rupture time is negligible. At this point the time step is fixed and the spatial grid is refined in a similar way to determine a rupture time which is independent of the mesh size. To illustrate this we consider the isothermal case, using rescaled spatial dimension X and time T, as detailed in §7. We follow Williams & Davis (1982) and divide the wavelength $\lambda = 2\pi/k$ into $N = 10$ equal elements of width $\Delta X = \lambda/10$, where $k = 2^{-\frac{1}{2}}$ is the maximizing wavenumber of linear theory. With this spatial grid fixed, we solve the (rescaled) evolution equation (7.3) using time steps $\Delta T = 0.1, 0.04$, 0.01 and 0.001 and find rupture times $T_R = 5.7, 5.64, 5.62$ and 5.611, respectively. We see that, for $\Delta T < 0.01$, the rupture time is not very sensitive to the time step. We use $\Delta T = 0.01$ and increase N until the computed rupture time no longer depends on the spatial grid. Figure 3 indicates that spatial-mesh effects become unimportant when $N > 20$.

In the following sections we detail numerical results for an isothermal film and for quasi-equilibrium and non-equilibrium evaporation and condensation. In each case we divide the disturbance wavelength into $N = 30$ equal elements, unless otherwise indicated. We employ a maximum time step $\Delta T = 0.01$, but use smaller time steps near rupture. Specifically, when the minimum film thickness is less than (0.65, 0.3, 0.1, 0.005), we take ΔT equal to (0.001, 0.0002, 0.0001, 0.00001), respectively.

We note that the values of the non-dimensional parameters which we use in our computations are *not* intended to be *physically realistic*; rather, they allow us to distinguish different physical effects and examine their interactions.

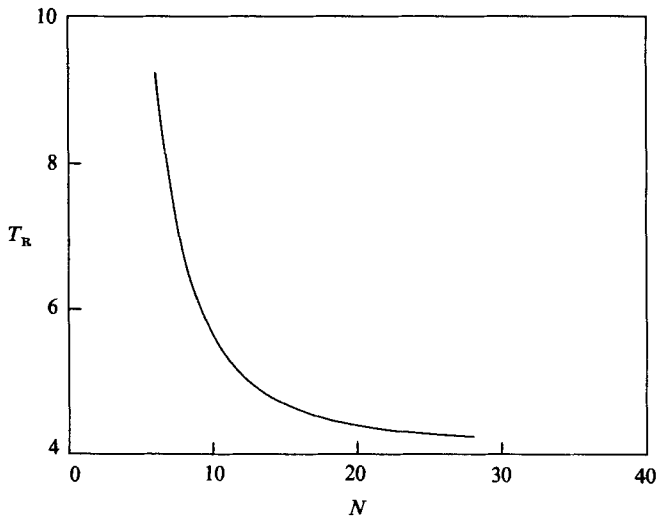

FIGURE 3. Rupture time T_R *vs.* spatial mesh size for the isothermal case. The time step is fixed at $\Delta T = 0.01$. The disturbance wavelength $\lambda = 2\pi\sqrt{2} = 8.88$ is divided into N equal elements, $N = \lambda/\Delta X$.

7. Isothermal film

Consider the case when $\bar{A}, \bar{S} = O(1)$, and $\bar{E}, \bar{E}^2\bar{D}^{-1} = o(1)$ with $K = 0$. The leading-order problem reduces to that posed by Williams & Davis (1982) for an isothermal static film subject to van der Waals attractions and constant surface tension. The resulting nonlinear evolution equation governing long-wave interfacial disturbances is then

$$h_t + A(h^{-1}h_x)_x + S(h^3 h_{xxx})_x = 0, \tag{7.1}$$

where $Ak, Sk^3 = O(1)$. The parameters A and S can be removed from (7.1) by rescaling. We write

$$X = (A/S)^{\frac{1}{2}}x, \quad T = (A^2/S)t, \tag{7.2a,b}$$

and obtain the canonical form

$$h_T + (h^{-1}h_X)_X + (h^3 h_{XXX})_X = 0. \tag{7.3}$$

Note that X and T are non-dimensional length and time variables related to their respective dimensional counterparts by scales $(A/S)^{\frac{1}{2}}d_0$ and $(A^2/S)(\nu/d_0^2)$.

We employ linear stability theory and perturb the base state $\bar{h} = 1$ by a small amount h'. We assume normal modes for the disturbance quantity h' of the form

$$h'(X,T) = H(T)\,\mathrm{e}^{\mathrm{i}kX}. \tag{7.4}$$

The resulting ordinary differential equation for the normal-mode amplitude H is

$$\dot{H}/H = k^2(1-k^2), \tag{7.5}$$

where the dot denotes the derivative, $\dot{H}/H$ is the growth rate, and k is the disturbance wavenumber. The cutoff wavenumber $k = k_C$ is given by $\dot{H}/H = 0$, so

$$k_C^2 = 1 \tag{7.6}$$

and small disturbances grow for all $0 < k < k_C$. Note from the scaling (7.2*a*) and definitions (3.3*b*) and (3.13) that k_C is independent of the viscosity of the liquid.

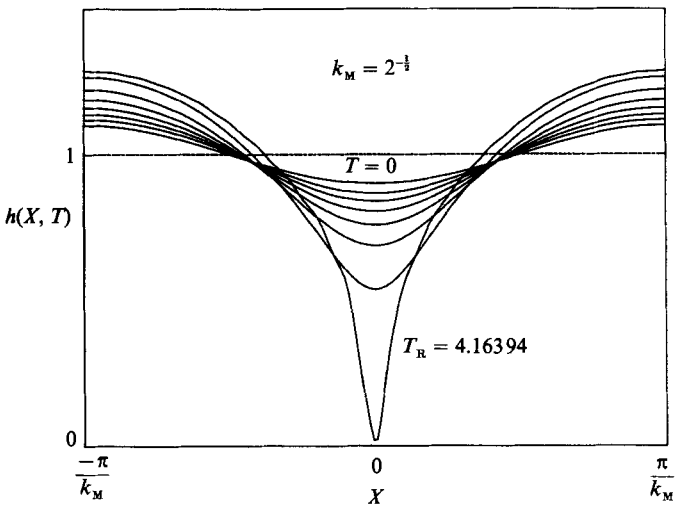

FIGURE 4. Film profiles at different times for the isothermal case.

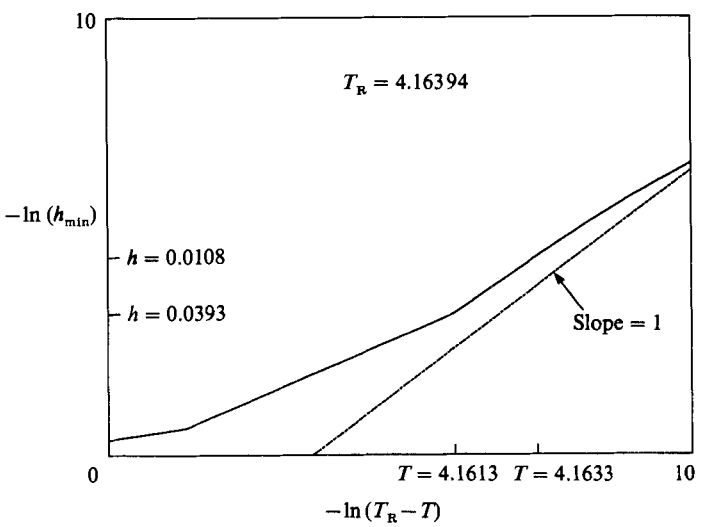

FIGURE 5. Local behaviour near rupture for the isothermal case.

Figure 4 shows a numerical solution to (7.3) on the interval $-\pi/k_M < X < \pi/k_M$, where $k_M = k_C/\sqrt{2}$ is the maximizing wavenumber of linear theory and we use the initial condition

$$h(X, 0) = 1 + 0.1 \sin(k_M X). \tag{7.7}$$

We employ $N = 40$, $\Delta T \leqslant 0.001$, and compute a rupture time $T_R = 4.2$. If we follow Williams & Davis (1982) and use $N = 10$, $\Delta T = 0.01$, we find $T_R = 5.6$, which compares favourably with the Williams/Davis result, $T_R = 5.7$. However, figure 3 indicates that the computed rupture time is sensitive to the spatial grid when $N = 10$, but when $N = 40$ it is not; $T_R = 4.2$ is more accurate.

As time $T \to T_R$, $h \to 0$, as shown in figure 4, and (7.3) is singular. We investigate this singularity and plot $-\ln(T_R - T)$ *vs.* $-\ln(h_{min})$, as shown in figure 5. We find that as time T increases from 4.1613 to 4.1633 (by time steps of 0.00001) the minimum film

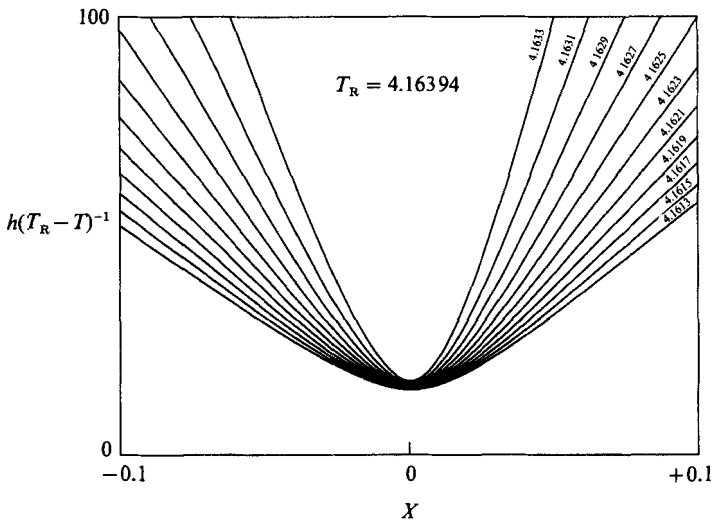

FIGURE 6. Local 'similarity' film profiles for the isothermal case.

thickness $h_{\min}$ decreases from 0.0393 to 0.0108. During this period near rupture the plotted curve has slope near unity, indicating that the minimum film thickness varies nearly linearly with time. Later in time this slope deviates significantly from unity.

We now plot $h(T_R - T)^{-1}$ *vs.* X, as shown in figure 6, for a time period inclusive of the above-mentioned region of nearly linear behaviour. We note that the film profiles, and consequently these 'similarity' profiles, are slightly asymmetric at late times. This is most likely due to numerical instability encountered as the coefficient matrix becomes nearly singular near rupture; at that point the numerics break down, as suggested by wiggles in the late-time profile of figure 4. These oscillations have been minimized by reducing the mesh size. We see that the minimum point for each profile in figure 6 remains in about the same position, so we conclude that near $T = T_R$ the local behaviour is almost like

$$h \approx k(T_R - T)\, F(X), \tag{7.8}$$

where the function $F(X)$ must be symmetric about $X = 0$. Notice that (7.8) is a solution of (7.1) when surface tension is negligible,

$$h_t + A(h^{-1}h_x)_x = 0, \tag{7.9}$$

subject to the condition at $x = 0$:

$$h_x = 0. \tag{7.10}$$

From (5.15) and (5.16) we have for the isothermal case the (leading-order) X-component of velocity

$$u \approx (h^{-3} - 3h_{XX})_X\, (\tfrac{1}{2}Z^2 - hZ), \tag{7.11}$$

where we have rescaled according to (7.2) with $Z = z$. From (7.8) and (7.11) we see that as $T \to T_R$, $Z \approx h$, and $u \approx (T_R - T)^{-1}$ so that the inertia neglected from (5.5) and (5.6) must become important just before rupture. Our evolution equation is only valid if inertia is negligible, which means that

$$k(u_T + uu_X + wu_Z) \approx k(T_R - T)^{-2} \ll 1, \tag{7.12a}$$

or

$$T_R - T \gg k^{\frac{1}{2}}. \tag{7.12b}$$

If one wants to follow the result *to* rupture, one must incorporate inertia into the evolution equation. We shall be content here to ignore inertia and analyse only as far as condition (7.12) allows. The slope of the curve in figure 5 departs from unity at late times; this may be related to the numerical instability mentioned above, but this can be ignored in light of (7.12).

Note that the numerical value reported here for the rupture time is not accurate to the number of digits shown in figure 5. We show the actual value used since the computations leading to the result shown in figure 5 are sensitive to T_R. When comparing our results with previous work we retain only two significant digits, since that is the most accuracy we could expect if the physical values of table 1 were employed. Also, the maximum time step (in this case $\Delta T = 0.001$) limits the precision of our computations. Naturally, figure 5 contains some uncertainty since numerical instability and our neglect of inertia at late times can both affect the computed rupture time.

8. Quasi-equilibrium evaporation ($K = 0$)

In extending the nonlinear theory to the case of an evaporating heated film, we again take $\bar{A}, \bar{S} = O(1)$, but now assume that $\bar{E}, \bar{D} = O(1)$. We consider first the quasi-equilibrium case and take $K = 0$ so that the interfacial temperature is constant and equal to its saturation value. The analysis again includes van der Waals attractions and surface tension, but is modified to account for the mass, momentum and energy transport of the evaporation process. Thus we include the added effects of mass loss, vapour recoil, and cooling due to the loss of latent heat. When $K = 0$ the temperature difference across the film is constant, so that the heat flux and thus the evaporation rate are expected to be larger where the film is thinner (cf. Bankoff 1971). Thus the vapour recoil is greater at the troughs than at the crests of the waves and clearly destabilizes the layer. Since we now consider a non-isothermal film we must solve the energy equation in the liquid, subject to the thermal condition at the interface and the constant-temperature boundary conditions.

We set $K = 0$ in (5.18) and obtain

$$h_t + Eh^{-1} + [(Ah^{-1} + E^2 D^{-1})\, h_x]_x + S(h^3 h_{xxx})_x = 0, \tag{8.1}$$

where Ak, Sk^3, Ek^{-1} and $Dk^{-3} = O(1)$. The term proportional to E in (8.1) measures the mass loss during evaporation while that proportional to E^2 derives from the vapour recoil. The parameters A and S can be removed from (8.1) by again rescaling according to (7.2). We obtain the general form

$$h_T + \mathscr{E} h^{-1} + [(h^{-1} + \mathscr{D})\, h_X]_X + (h^3 h_{XXX})_X = 0, \tag{8.2}$$

where

$$\mathscr{E} = ES/A^2, \quad \mathscr{D} = E^2 D^{-1} S/A^2. \tag{8.3a,b}$$

Equation (8.2) is not satisfied by h being constant owing to mass loss. The basic state is a thinning static layer, which is X-independent, and whose thickness $\bar{h} = \bar{h}(T)$ is given by the leading-order expression

$$\bar{h} = (1 - 2\mathscr{E}T)^{\frac{1}{2}}. \tag{8.4}$$

The layer has depth unity at time zero and disappears in a finite time $T = T_D = 1/2\mathscr{E}$. The slowly varying assumptions that lead to (8.2) break down near $T = 0$ and $T = T_D$, as discussed in §4.1; (8.2) holds only in the (long) excluded interval.

We employ linear stability theory and perturb the base state $\bar{h}$ by a small amount h'. We use normal modes of the form (7.4) and obtain an ordinary differential equation for the normal-mode amplitude H:

$$\dot{H}/H = \mathscr{E}\bar{h}^{-2} + (\bar{h}^{-1} + \mathscr{D})\,k^2 - \bar{h}^3 k^4. \tag{8.5}$$

The full dynamic behaviour of the perturbed basic state is then described by

$$H = H_0\,\bar{h}^{-1} \exp\left\{\frac{k^2}{\mathscr{E}}\left[(1-\bar{h}) + \tfrac{1}{2}\mathscr{D}(1-\bar{h}^2) - \tfrac{1}{5}k^2(1-\bar{h}^5)\right]\right\}, \tag{8.6}$$

where we use solution (8.4) for $\bar{h}$. The term $\mathscr{E}\bar{h}^{-2}$ in (8.5) results from the mass loss and gives rise to the coefficient $\bar{h}^{-1}$ in (8.6). This algebraic behaviour, in contrast with the exponential behaviour elsewhere, does not influence the (exponential) instability. We may rewrite (8.6) in the equivalent form

$$H = H_0\,\bar{h}^{-1} \exp\left\{\frac{k^2(1-\bar{h})}{\mathscr{E}}\left[1 + \tfrac{1}{2}\mathscr{D}(1+\bar{h}) - \tfrac{1}{5}(\bar{h}^4 + \bar{h}^3 + \bar{h}^2 + \bar{h}^1 + 1)\,k^2\right]\right\}. \tag{8.7}$$

It is useful in interpretation to talk about an *effective growth rate* $\omega_E(T)$, defined as the exponent in (8.7) divided by time T. Figure 7 shows a plot of $\omega_E(T)$ *vs.* k^2. We find a range of unstable wavenumbers such that $0 < k^2 < k_C^2$. The cutoff wavenumber $k = k_C$ is given by $\omega_E(T) = 0$. We find that the maximum growth rate increases with time while the range of unstable wavenumbers gets wider: as $\mathscr{E}T \to 0$, $\omega_E \approx k^2(1 + \mathscr{D} - k^2)$ and $k_C^2 \to 1 + \mathscr{D}$, but as $\mathscr{E}T \to \mathscr{E}T_D$, $\omega_E \approx 2k^2(1 + \frac{1}{2}\mathscr{D} - \frac{1}{5}k^2)$ and $k_C^2 \to 5(1 + \frac{1}{2}\mathscr{D})$. The rupture instability is thus augmented by the evaporative effect of vapour recoil. We expect the unstable film to rupture at some time T_R earlier than the base-state disappearance time T_D.

Figures 8 and 9 show numerical solutions to (8.2). The computations are equivalent to those that produced figure 4 for the isothermal case except that quasi-equilibrium evaporation has been included in the analysis. We again consider a disturbance wavenumber

$$k_M = 2^{-\frac{1}{2}}, \tag{8.8}$$

which is the maximizing wavenumber from linear theory for the *isothermal case*. When $\mathscr{E} = 0.1$ and $\mathscr{D} = 1$, we find a rupture time $T_R = 1.1$, which is much less than the isothermal result, $T_R = 4.2$, and the film profile evolves as shown in figure 8. When $\mathscr{E} = \mathscr{D} = 1$, the film ruptures even sooner, at $T_R = 0.34$, and the film profile evolves as shown in figure 9. We see that the results are quite sensitive to the magnitude of the modified evaporation number $\mathscr{E}$.

We solve the unrescaled equation (8.1) to obtain figures 10 and 11. Figure 10 shows the interaction between quasi-equilibrium mass loss and vapour recoil when long-range forces are negligible ($A = 0$) and $3S = 1$, $k_M = (3/2)^{\frac{1}{2}}$. When evaporation is also negligible ($E = E^2D^{-1} = 0$) surface tension stabilizes the film. When $E = 0.1$, $E^2D^{-1} = 0$, the film ruptures at $t_R = 4.76$ due solely to mass loss. When $E = 0$, $E^2D^{-1} = 1$, vapour recoil destabilizes the film, causing rupture at $t_R = 2.01$. With both mass loss and vapour recoil included ($E = 0.1$, $E^2D^{-1} = 1$) the film ruptures earliest, at $t_R = 1.38$.

Figure 11 shows the effects of quasi-equilibrium evaporation on the minimum film thickness when van der Waals attractions are important. We take $A = 3S = 1$, and $k_M = (A/2S)^{\frac{1}{2}}$, and consider variations in E and D. When evaporation is negligible ($E = E^2D^{-1} = 0$) the isothermal case is retrieved, with rupture occurring at $t_R = 1.46$. When $E = 0.1$, $E^2D^{-1} = 0$, only mass loss is added to the analysis, and the thinning

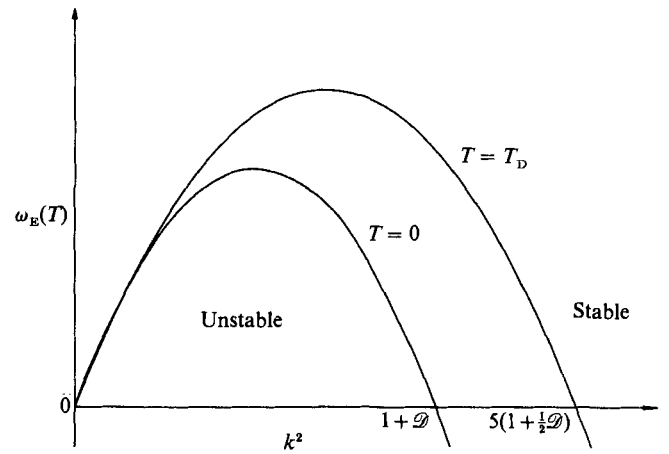

FIGURE 7. Linear stability results showing the growing range of unstable wavenumbers for quasi-equilibrium evaporation.

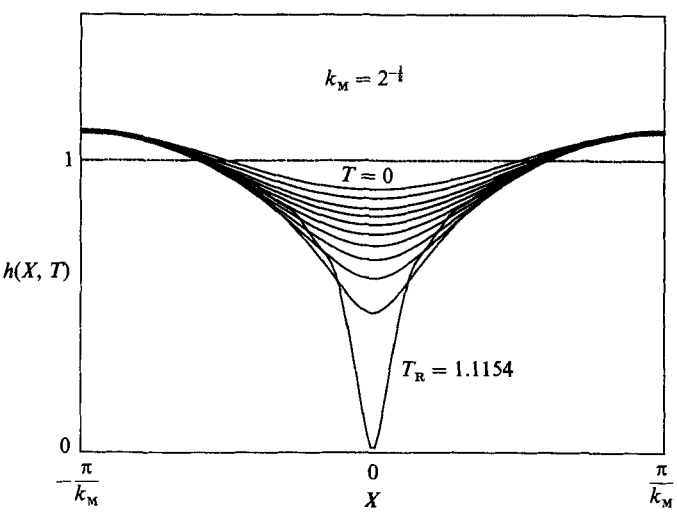

FIGURE 8. Film profiles at different times for quasi-equilibrium evaporation when vapour recoil is important ($\mathscr{D} = 1$) and mass loss is less important ($\mathscr{E} = 0.1$).

film ruptures sooner, at $t_R = 0.99$. When $E = 0, E^2D^{-1} = 1$, mass loss is negligible, but the destabilizing effect of vapour recoil accelerates rupture to $t_R = 0.55$. When both mass loss and vapour recoil are included ($E = 0.1, E^2D^{-1} = 1$) we have $t_R = 0.49$. In each case a comparison between figures 10 and 11 clearly illustrates the destabilizing effect of van der Waals attractions.

As time $T \to T_R$, $h \to 0$ and (8.2) is singular. We investigate this singularity and plot $-\ln(T_R - T)$ *vs.* $-\ln(h_{min})$ for several combinations of $\mathscr{E}$ and $\mathscr{D}$. When mass loss is absent and vapour recoil is present ($\mathscr{E} = 0, \mathscr{D} = 1$), figure 12 shows that near rupture this curve has slope near unity, indicating that the minimum film thickness varies nearly linearly with time. Closer to rupture the slope deviates from unity, but this is not worrisome since the reliability of our computations is in doubt when we get too close to the singularity at $h = 0$. We plot $h(T_R - T)^{-1}$ *vs.* X, as shown in figure 13, to

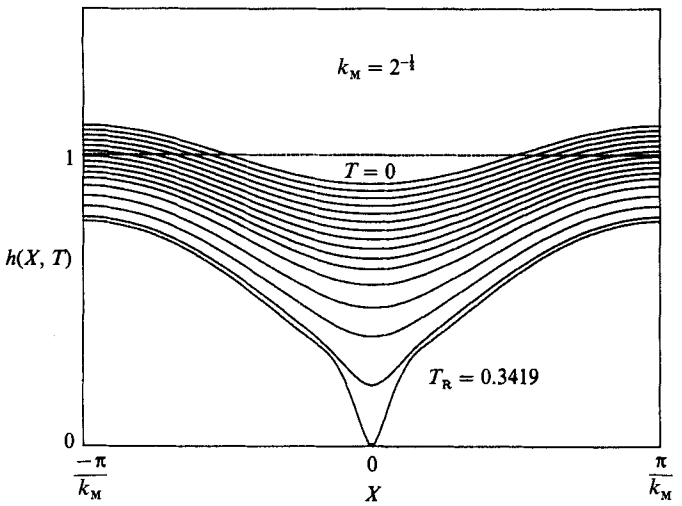

FIGURE 9. Film profiles at different times for quasi-equilibrium evaporation when vapour recoil and mass loss are both important ($\mathscr{D} = \mathscr{E} = 1$).

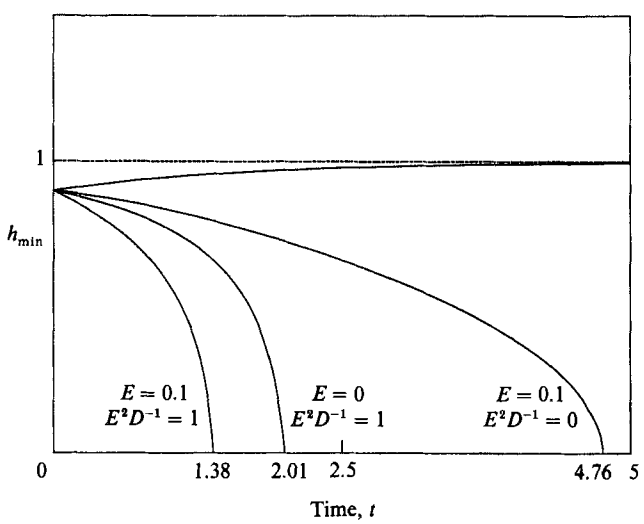

FIGURE 10. Minimum film thickness as a function of time, for various degrees of quasi-equilibrium mass loss and vapour recoil, when long-range molecular forces are negligible ($A = 0$, $S = \frac{1}{3}$).

illustrate the 'similarity' behaviour. In this case we conclude that near $T = T_R$ the local behaviour is again like

$$h = k(T_R - T)\,F(X), \tag{8.9}$$

where $F(X)$ is symmetric about $X = 0$. However, when mass loss is important ($\mathscr{E} = 1$) we find a slope near rupture of about 1/2, whether vapour recoil is present ($\mathscr{D} = 1$) or not ($\mathscr{D} = 0$). This indicates that the local behaviour is now like

$$h \approx k(T_R - T)^{\frac{1}{2}}F(X). \tag{8.10}$$

This behaviour is nearly identical to the behaviour when the disturbance amplitude is zero (the basic state) as indicated by (8.4). When mass loss is present to a lesser degree ($\mathscr{E} = 0.1$), and vapour recoil is still important ($\mathscr{D} = 1$), the competing effects result in a slope near rupture of about 2/3.

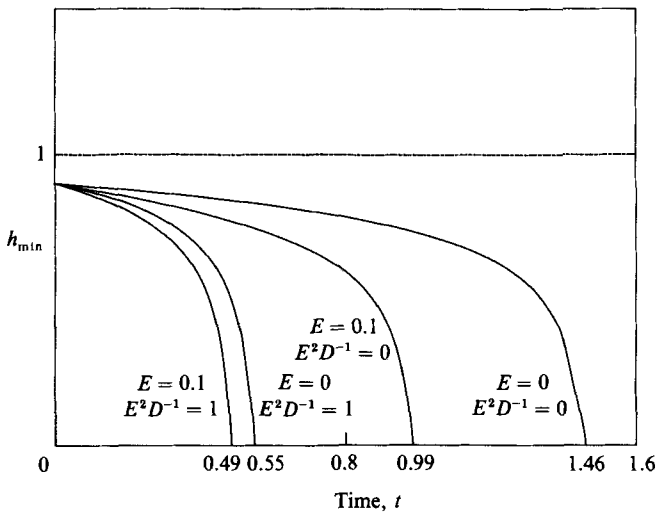

FIGURE 11. Minimum film thickness as a function of time, for various degrees of quasi-equilibrium mass loss and vapour recoil, when long-range molecular forces are important ($A = 1$, $S = \frac{1}{3}$).

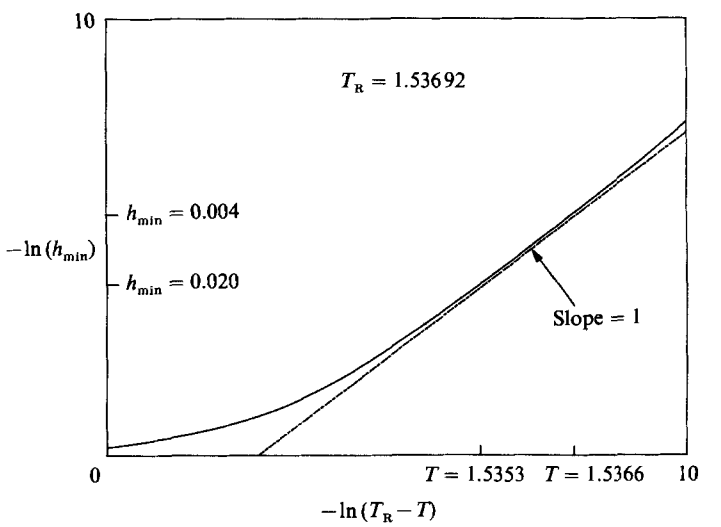

FIGURE 12. Local behaviour near rupture for quasi-equilibrium evaporation when mass loss is negligible ($\mathscr{E} = 0$) but vapour recoil is important ($\mathscr{D} = 1$).

9. Non-equilibrium evaporation ($K \neq 0$)

We now allow $K \neq 0$ so as to extend (8.1) to non-equilibrium evaporation. In this case the interface temperature depends on the fluxes. We again take $\bar{A}, \bar{S}, \bar{E}, \bar{D} = O(1)$, and also assume $P, K, \bar{M} = O(1)$ to retain thermocapillarity. We have the evolution equation (5.18):

$$h_t + E(h+K)^{-1} + S(h^3 h_{xxx})_x + \{[Ah^{-1} + E^2 D^{-1}(h+K)^{-3}h^3 + KMP^{-1}(h+K)^{-2}h^{-2}]h_x\}_x = 0, \quad (9.1)$$

where $Ak, Sk^3, Ek^{-1}, Dk^{-3}$ and $Mk = O(1)$. The term proportional to M represents the thermocapillary effect, which is present since the interface now has non-uniform

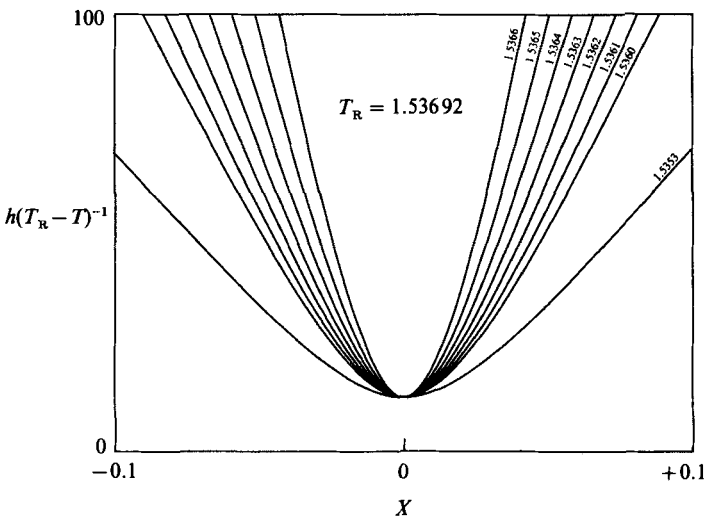

FIGURE 13. Local 'similarity' film profiles for quasi-equilibrium evaporation when mass loss is negligible ($\mathscr{E} = 0$) but vapour recoil is important ($\mathscr{D} = 1$).

temperature. After rescaling according to (7.2) to remove the parameters A and S we obtain

$$h_T + \mathscr{E}(h+K)^{-1} + (h^3 h_{XXX})_X + \{[h^{-1} + \mathscr{D}(h+K)^{-3}h^3 + K\mathscr{M}(h+K)^{-2}h^2]\, h_X\}_X = 0, \tag{9.2}$$

where $\mathscr{E}$ and $\mathscr{D}$ are given by (8.3) and

$$\mathscr{M} = MP^{-1}S/A^2. \tag{9.3}$$

Equation (9.2) reduces to (8.2) in the limit $K \to 0$, while in the limit $K^{-1} \to 0$ (the non-volatile case) (7.3) is retrieved.

The basic state is again a thinning static layer which is X-independent. In this case the leading-order expression for the basic-state film thickness is

$$\bar{h} = -K + (K^2 + 2K + 1 - 2\mathscr{E}T)^{\frac{1}{2}}. \tag{9.4}$$

The layer disappears in a finite time $T = T_D = (1+K)^2/2\mathscr{E}$, and the slowly varying assumptions again break down near $T = 0$ and $T = T_D$.

We again examine linear stability of the base state, using normal modes of the form (7.4), and find the following ordinary differential equation for the normal-mode amplitude H:

$$\dot{H}/H = \mathscr{E}(\bar{h}+K)^{-2} - (\bar{h})^3 k^4 + [(\bar{h})^{-1} + \mathscr{D}(\bar{h}+K)^{-3}(\bar{h})^3 + K\mathscr{M}(\bar{h}+K)^{-2}(\bar{h})^2]\, k^2. \tag{9.5}$$

The full dynamic behaviour of the perturbed basic state is quite complicated:

$$H = H_0 \left[\left(\frac{1+K}{\bar{h}+K}\right)^{[1+(3K^2\mathscr{D}+K^3\mathscr{M})k^2/\mathscr{E}]} (\bar{h})^{-Kk^2/\mathscr{E}}\right] \exp\left\{\frac{k^2(1-\bar{h})}{\mathscr{E}}\left[1 - \tfrac{1}{5}k^2(1+\bar{h}+\bar{h}^2+\bar{h}^3+\bar{h}^4)\right.\right.$$
$$\left.\left. - \tfrac{1}{4}k^2K(1+\bar{h}+\bar{h}^2+\bar{h}^3) - 3K\mathscr{D} + 2K\mathscr{M} - \frac{K^3\mathscr{D}}{(\bar{h}+K)(1+K)} + \tfrac{1}{2}(\bar{h}+2K+1)(\mathscr{D}+K\mathscr{M})\right]\right\}. \tag{9.6}$$

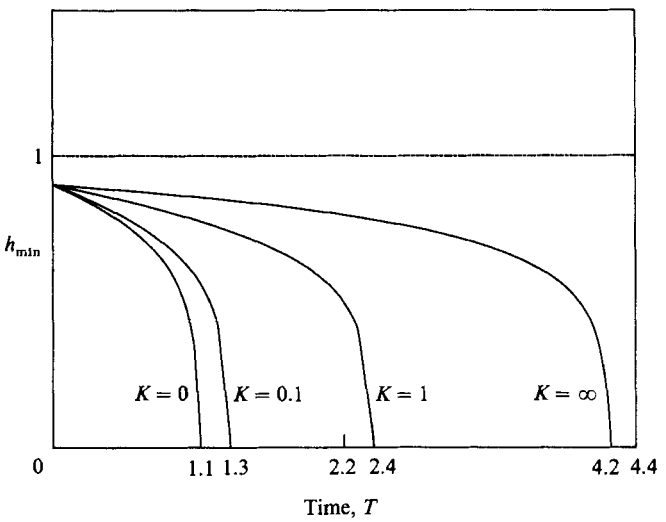

FIGURE 14. Minimum film thickness as a function of time for various degrees of non-equilibrium evaporation when some mass loss is present ($\mathscr{E} = 0.1$) and vapour recoil is important ($\mathscr{D} = 1$) but thermocapillarity is negligible ($\mathscr{M} = 0$).

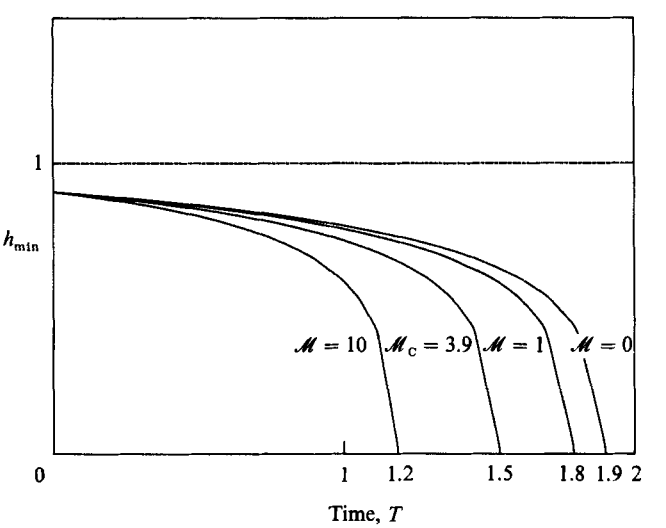

FIGURE 15. Minimum film thickness as a function of time for various degrees of thermocapillarity due to non-equilibrium evaporation ($K = 0.1$) when vapour recoil is important ($\mathscr{D} = 1$) but mass loss is negligible ($\mathscr{E} = 0$).

The mass-loss effect again enters algebraically, giving rise to the coefficient $(1+K)/(\bar{h}+K)$; it does not influence the (exponential) instability. The dimensionless groups $\mathscr{E}$, $\mathscr{D}$, $\mathscr{M}$ and K influence the algebraic behaviour, appearing as exponents which modify the above coefficient. Relative to the quasi-equilibrium result, the effective growth rate is *either increased or decreased*, depending on the relative magnitudes of the dimensionless groups.

Figure 14 shows how different degrees of non-equilibrium affect the evaporating film when thermocapillary effects are neglected. As K increases, the layer becomes less volatile and thus takes longer to rupture. (When $K \to \infty$, the non-volatile case is

retrieved). When thermocapillarity is important, the rupture time may be greater or less than for the quasi-equilibrium case, as shown in figure 15 for the case when mass loss is neglected ($\mathscr{E} = 0$) but vapour recoil is important ($\mathscr{D} = 1$). When $K = 0.1$, $\mathscr{M} = 3.9$, the rupture time $T_R = 1.5$ coincides with the rupture time for the quasi-equilibrium case ($K = 0$). We see that non-equilibrium effects destabilize relative to the quasi-equilibrium result when $\mathscr{M}$ is larger than this critical value $\mathscr{M}_C = 3.9$. When $\mathscr{M} < \mathscr{M}_C$, stabilization of the rupture and vapour recoil instabilities overcompensates for the destabilizing effect of thermocapillarity; this results in a net stabilization relative to the quasi-equilibrium result.

As time $T \to T_R$, $h \to 0$, and (9.2) is singular. We investigate this singularity and plot $-\ln(T_R - T)$ *vs.* $-\ln(h_{min})$ for each of the cases shown in figures 14 and 15. The case of quasi-equilibrium evaporation ($K = 0$) results in a curve of slope near 2/3 as T approaches T_R. Each of the other cases result in a slope near unity.

10. Condensation

Suppose that instead of a heated plate we consider a cooled plate maintained at a constant temperature T_C, where T_C is less than the saturation temperature T_S. This is the case of condensation, or 'negative evaporation'. We take T_C as a reference and scale the temperature difference $T - T_C$ on the temperature difference $\Delta T = T_S - T_C$. For condensation the mass flux is negative; it is again scaled on $k\Delta T/d_0 L$. The temperature boundary condition at the solid surface (3.6*b*) is now

$$T = 0. \tag{10.1}$$

At the interface the constitutive equation (3.17) becomes

$$KJ = T - 1. \tag{10.2}$$

The base state is a thickening static layer which is x-independent. The leading-order basic-state solution is

$$\bar{h} = -K + (K^2 + 2K + 1 + 2Et)^{\frac{1}{2}}, \tag{10.3a}$$

$$\bar{T} = (K^2 + 2K + 1 + 2Et)^{-\frac{1}{2}} z, \tag{10.3b}$$

$$\bar{J} = -(K^2 + 2K + 1 + 2Et)^{-\frac{1}{2}}, \tag{10.3c}$$

$$\bar{p} = \tfrac{3}{2} E^2 D^{-1} (K^2 + 2K + 1 + 2Et)^{-1}. \tag{10.3d}$$

A long-wave analysis yields a slightly modified form of (5.18):

$$h_t - E(h+K)^{-1} + S(h^3 h_{xxx})_x + \{[Ah^{-1} + E^2 D^{-1}(h+K)^{-3} h^3 - KMP^{-1}(h+K)^{-2} h^2] h_x\}_x = 0, \tag{10.4}$$

where E and M are again defined to be positive. If we now redefine $\mathscr{E}$ and $\mathscr{M}$ as negative quantities

$$\mathscr{E} = -ES/A^2, \quad \mathscr{M} = -MP^{-1}S/A^2, \tag{10.5a,b}$$

and rescale (10.4) according to (7.2), then the result is identical to (9.2).

We consider the case of quasi-equilibrium condensation ($K = 0$) and examine linear stability theory. The full dynamic behaviour of the perturbed basic state is again described by (8.7). However, for condensation $\mathscr{E}$ is negative, so that as time increases the layer becomes more stable. Figure 16 illustrates how the cutoff wavenumber decreases with time, thus shrinking the unstable range and reducing the maximum growth rate. Figure 17 shows a numerical solution of (10.4) with $k_M = (3/2)^{\frac{1}{2}}$. In this case the stabilizing effects of mass gain and thermocapillarity are

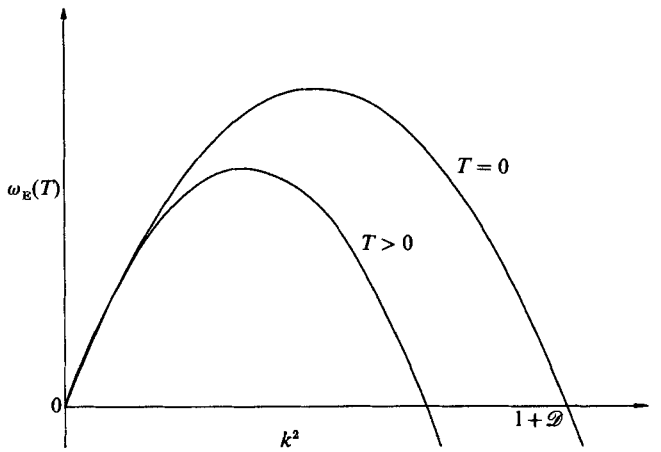

FIGURE 16. Linear stability results showing the shrinking range of unstable wavenumbers for quasi-equilibrium condensation.

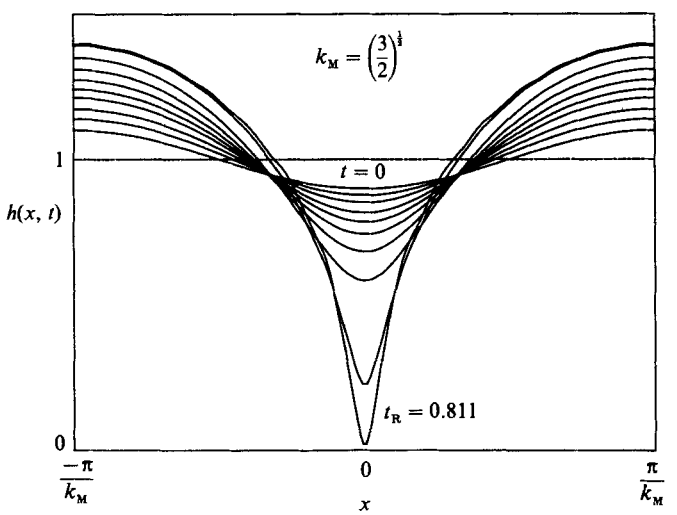

FIGURE 17. Film profiles at different times for non-equilibrium condensation including mass gain ($E = -0.1$), vapour recoil ($E^2D^{-1} = 1$) and thermocapillarity ($MP^{-1} = -1$). $A = 1$, $S = \frac{1}{3}$, $K = 0.1$.

included, but they still lose the competition with the vapour recoil and rupture instabilities. The film ruptures at time $t_R = 0.8$, which is still earlier than the isothermal rupture time ($t_R = 1.4$) but later than if mass gain and thermocapillary effects were negligible ($t_R = 0.5$).

Figure 18 compares evaporation and condensation results when mass loss/gain is negligible. Since vapour recoil is destabilizing in either case, when $K = 0$ (quasi-equilibrium) both cases lead to rupture at $T_R = 1.5$. Similarly, when $K = 0.1$ and thermocapillary effects are neglected ($\mathscr{M} = 0$) both cases lead to rupture at $T_R = 1.9$. However, the inclusion of thermocapillary effects delays rupture in the condensation case ($\mathscr{M} = -1$, $T_R = 2.0$) but accelerates rupture in the evaporation case ($\mathscr{M} = 1$, $T_R = 1.8$). This makes sense physically since surface tension induces a flow directed from warmer to cooler regions. For condensation the troughs are cooler than the

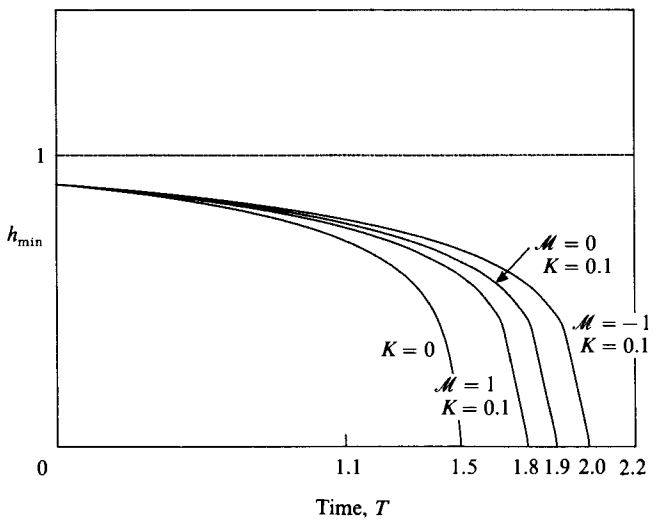

FIGURE 18. Minimum film thickness as a function of time, comparing non-equilibrium evaporation and condensation when mass loss is negligible ($\mathscr{E} = 0$) but vapour recoil is not ($\mathscr{D} = 1$).

crests and tend to be 'filled in'. For evaporation the direction of this induced flow is reversed. For each case shown in figure 18, the local behaviour near rupture is like

$$h \approx k(T_R - T)\, F(X). \tag{10.6}$$

11. Quasi-steady linear stability theory

The stability of systems with interfacial phase change has always been examined using quasi-steady stability theory (Palmer 1976; Prosperetti & Plesset 1984) when the basic state is unsteady, or quasi-parallel theory (cf. Bankoff 1971; Marschall & Lee 1973; Unsal & Thomas 1978; Spindler 1982) when the basic state involves mean flow and the layer grows or decays in the downstream direction. In the former case the approximation supposes that in analysing the stability of a time-dependent basic state, that the basic state varies slowly compared with the growth rate of disturbances so that one can freeze the basic state at an instant and examine its stability as if it were a steady state (Davis 1976). We wish to evaluate this approach for the present case and consider first the case of quasi-equilibrium evaporation or condensation.

If we assume quasi-steady behaviour and take $\bar{h} = 1$, the basic-state value at $t = 0$, this *frozen base state* does not depend on time, and (8.5) becomes

$$\dot{H}/H = \mathscr{E} + (1 + \mathscr{D})\, k^2 - k^4, \tag{11.1}$$

and the cutoff wavenumber k_C is given by

$$k_C^2 = \frac{(1+\mathscr{D}) + [(1+\mathscr{D})^2 + 4\mathscr{E}]^{\frac{1}{2}}}{2}. \tag{11.2}$$

Equations (11.1) and (11.2) are valid for either evaporation or condensation, $\mathscr{E}$ being either positive or negative, respectively. Figure 19 illustrates how the growth rate $\dot{H}/H$ varies with k^2; when $\mathscr{E}$ is positive (negative) (11.1) yields the top (bottom) curve. The mass-loss (gain) term appears here as an artifact since what should be an

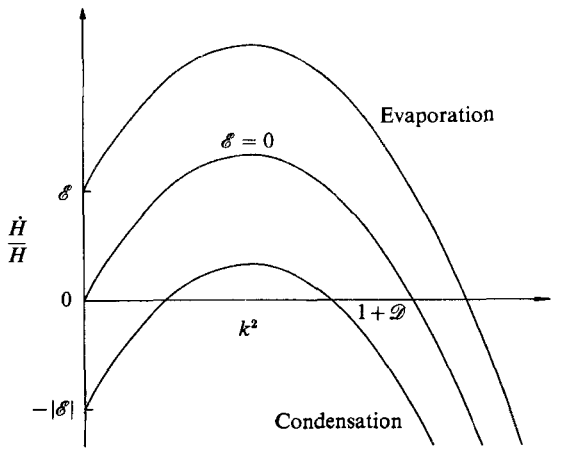

FIGURE 19. Quasi-steady linear stability behaviour for evaporation and condensation showing how mass loss/gain shifts the growth rate curve.

algebraic contribution to the disturbance amplitude is seen here as an exponential one. For the evaporation case this reflects the fact that by quasi-steady theory even if the interface is undisturbed (i.e. $k = 0$) the film is still strongly 'unstable'. In actuality, the film is merely thinning and this thinning is properly part of the basic state. Similarly, for the condensation case the undisturbed film is 'stabilized' by thickening. When the mass-loss (gain) term is not included ($\mathscr{E} = 0$), but vapour recoil is retained ($\mathscr{D} \neq 0$), then (11.2) becomes

$$k_C^2 = 1 + \mathscr{D} \tag{11.3}$$

for both evaporation and condensation, and (11.1) yields the middle curve in figure 19. The quasi-steady approximation yields an artifact, in that at $k = 0$ it predicts strong instability (stability) for the case of mass loss (gain) whereas the proper time-dependent theory gives neutral conditions at $k = 0$ as seen in figures 7 and 16. Note that the errors produced by the quasi-steady approximation are largest where disturbances, assumed to be rapidly growing, are actually neutral, viz. near $k = 0$ and $k = k_C$.

Consider now the case of non-equilibrium evaporation or condensation. We again assume quasi-steady behaviour and take $\bar{h} = 1$. Equation (9.5) becomes

$$\dot{H}/H = \mathscr{E}(1+K)^{-2} + [1 + \mathscr{D}(1+K)^{-3} + K\mathscr{M}(1+K)^{-2}]k^2 - k^4. \tag{11.4}$$

The mass-loss (gain) term again appears as an artifact. If it is neglected ($\mathscr{E} = 0$), then the critical wavenumber is given by

$$k_C^2 = 1 + \mathscr{D}(1+K)^{-3} + K\mathscr{M}(1+K)^{-2}. \tag{11.5}$$

Note that non-equilibrium evaporation ($K \neq 0$, $\mathscr{M} > 0$) weakens the destabilizing effect of vapour recoil, but introduces a thermocapillary instability. Non-equilibrium condensation ($K \neq 0$, $\mathscr{M} < 0$) also weakens the vapour-recoil instability, but now introduces a stabilizing thermocapillary effect.

For $K = o(1)$, equation (11.4) can be approximated to order K as

$$\dot{H}/H = (1-2K) + [1 + \mathscr{D}(1-3K) + K\mathscr{M}]k^2 - k^4. \tag{11.6}$$

For evaporation ($\mathscr{M} > 0$) equation (11.6) clearly illustrates the competition between thermocapillarity and non-equilibrium vapour recoil. If mass loss is neglected, (11.6) reduces to the quasi-equilibrium result when $\mathscr{M} = 3\mathscr{D}$. Thus, for small K, linear theory predicts a critical value $\mathscr{M}_{\mathrm{C,L}} = 3\mathscr{D}$. Solution of the full nonlinear evolution equation (9.2) with $\mathscr{E} = 0$ and $K = 0.1$ (figure 15) yields a critical value $\mathscr{M}_{\mathrm{C,N}} = 3.9\mathscr{D}$. Thus, when $3.0 < \mathscr{M}/\mathscr{D} < 3.9$, quasi-steady linear theory predicts the thermocapillary effect to be destabilizing, but according to nonlinear theory it is stabilizing. We conclude that nonlinearity is stabilizing with respect to thermocapillarity.

12. Constant heat flux

Finally, we consider the case in which the bounding plate has a fixed heat flux, rather than a fixed temperature, and again allow for evaporative, thermocapillary and rupture instabilities. If we use the same formalism as in §5, we can derive the appropriate (rescaled) evolution equation:

$$h_T + \mathscr{E} + (h^{-1}h_X)_X + (h^3 h_{XXX})_X = 0. \tag{12.1}$$

Now, however, vapour recoil and thermocapillarity do not appear because it turns out that the mass flux and temperature are constant along the interface. For evaporation $\mathscr{E}$ is positive, and the liquid temperature is given by

$$T_0 = K + h - z. \tag{12.2}$$

The interfacial temperature is $T^{(\mathrm{I})} = K$, and the temperature at the heated boundary varies as $T_{\mathrm{H}} = K + h$ to accommodate the fixed linear temperature profile across the perturbed layer. For condensation $\mathscr{E}$ is negative, and the liquid temperature is given by

$$T_0 = -K - h + z. \tag{12.3}$$

The interfacial temperature is now $T^{(\mathrm{I})} = -K$, and the temperature at the cooled boundary varies as $T_{\mathrm{C}} = -K - h$. In each case the base-state film thickness is given by the leading-order expression

$$\bar{h} = 1 - Et. \tag{12.4}$$

Clearly the film bounded by a constant-temperature solid surface is more susceptible to instabilities driven by non-equilibrium phase change than is the layer on a fixed-flux surface.

13. Discussion and conclusions

We consider a thin viscous liquid layer bounded above by its vapour and below by a uniformly heated (cooled) rigid plane. We concentrate on a limiting case of the two-fluid problem so as to decouple the dynamics of the vapour from the dynamics of the liquid. This yields what we call the *one-sided model* of evaporation (condensation). We consider long-wave disturbances and derive a strongly nonlinear evolution equation (5.18) which governs the stability of the liquid layer subject to various coupled mechanisms. These include mass loss (gain), vapour recoil, thermocapillarity, long-range molecular forces, surface tension, and viscous forces. Equation (5.18) represents a major step in the description of evaporating (condensing) films. Rather than having to solve the free-boundary problem described in §2, we need only solve the single partial differential equation (5.18), subject to initial conditions. We analyse both linear and nonlinear stability of the liquid layer according to (5.18), using numerical methods in the latter case. Our aim is to distinguish different

physical effects and examine their interactions; the non-dimensional parameter values which are used in the discussion are not necessarily physically realistic.

We consider first the case of an isothermal static film subject to van der Waals attractions and constant surface tension. A linear stability analysis of the steady base state $\bar{h} = 1$ yields a fixed range of wavenumbers for which small disturbances grow. We compute a nonlinear rupture time which agrees well with that reported by Williams & Davis (1982). However, when the spatial grid is refined to minimize mesh dependence, the computed rupture time is reduced by about 25%.

When evaporation is considered, the base state is a thinning static layer. A linear stability analysis of this time-dependent base state yields a time-dependent range of unstable wavenumbers. We define an effective growth rate which excludes the algebraic contribution of mass loss. As the film thins, the maximum effective growth rate increases while the range of unstable wavenumbers gets wider. The rupture instability is thus augmented by the vapour-recoil instability.

When non-equilibrium evaporation is considered, the interfacial temperature depends on the fluxes and destabilizing thermocapillary effects appear. Non-equilibrium slows the mass loss, and consequently the vapour recoil, since, as the film thins, the interfacial temperature is allowed to increase toward that of *the heated* plate. A linear stability analysis of the basic state shows that the effective growth rate is either increased or decreased, with respect to the quasi-equilibrium result, depending on which effect wins the competition between non-equilibrium stabilization and thermocapillary destabilization. When thermocapillary effects are not important, an increase in the degree of non-equilibrium causes the layer to become less volatile and increases the rupture time.

When condensation is considered, the basic state is a static layer which grows thicker with time. For quasi-equilibrium condensation, a linear stability analysis of the base state again yields a time-dependent range of unstable wavenumbers. As the film thickens this range gets narrower, and the maximum effective growth rate decreases. When non-equilibrium effects are included, the mass gain is inhibited; this reduces the vapour-recoil instability. A linear stability analysis of the time-dependent base state shows that non-equilibrium decreases the effective growth rate relative to the quasi-equilibrium result.

Evaporation and condensation results are best compared when mass loss/gain is negligible. Under the quasi-equilibrium assumption, both cases lead to rupture at the same time, since vapour recoil is destabilizing for both. Under the non-equilibrium assumption, the cases lead to the same result if mass loss/gain and thermocapillarity are neglected. The inclusion of thermocapillarity delays rupture in the condensation case, but accelerates rupture in the evaporation case.

The above theory, by utilizing the long-wave nature of the instabilities, allows analysis of the instabilities of time-dependent basic states. If one compares these results with those using a quasi-steady stability theory, one can evaluate the latter. If we take the basic state as frozen at $\bar{h} = 1$ when examining linear theory, we find small-wavenumber artifacts arising. For both evaporation and condensation the mass loss/gain term gives rise to artifacts that result in vertical shifts in the growth rate curve relative to the case when mass loss/gain is neglected. For evaporation this indicates instability (i.e. positive growth rate) at zero wavenumber. For condensation it indicates stability (i.e. negative growth rate) for long waves. Neither interpretation is correct. Since the basic state is unsteady, it seems natural to compare the disturbance growth rate with the rate of change of the basic state (Shen 1961). The case when mass loss/gain is neglected yields a more correct linear stability result.

It appears that the local behaviour near rupture may be described by the 'similarity' form

$$h \approx k(t-t_{\mathrm{R}})^{q} F(x). \tag{13.1}$$

The exponent q has the value unity in those cases where mass loss is negligible, whereas $q = \frac{1}{2}$ when it is dominant. When mass loss is significant but not dominant, a value of q between $\frac{1}{2}$ and unity may be appropriate. We note that inertia becomes important just before rupture. Our analysis neglects inertia.

In the derivation of (5.18) we assume two-dimensional dynamics with $h = h(x, t)$. If, instead, we allow three-dimensional flow so that $h = h(x, y, t)$, then we can derive the three-dimensional equivalent to the evolution equation. Also, it is easy to account for the (stabilizing) effect of gravity. We assume that $\partial/\partial x$ and $\partial/\partial y$ are comparable, since the disturbance has no preferred direction, and find

$$h_t + E(h+K)^{-1} + \nabla\cdot[Sh^3\nabla(\nabla^2 h)] + \nabla\cdot\{[Ah^{-1} - Gh^3 + E^2D^{-1}(h+K)^{-3}h^3 + KMP^{-1}(h+K)^{-2}h^2]\nabla h\} = 0. \tag{13.2}$$

Here ∇ is the usual gradient operator in variables x and y, G is a non-dimensional measure of gravity g,

$$G = \frac{d_0^3 g}{3\nu^2}, \tag{13.3}$$

and buoyancy is considered negligible. Equation (13.2) corrects and extends the three-dimensional result presented by Williams & Davis (1982). The gravity term in (13.2) is identical to that given by Davis (1983) for a non-volatile heated film.

The authors gratefully acknowledge the support of the U.S. Department of Energy, Division of Basic Energy Sciences, through Grant no. DE FG02-86ER13641.

REFERENCES

Atherton, R. W. & Homsy, G. M. 1976 On the derivation of evolution equations for interfacial waves. *Chem. Engng Commun.* **2**, 57–77.

Bankoff, S. G. 1971 Stability of liquid flow down a heated inclined plane. *Intl J. Heat Mass Transfer* **14**, 377–385.

Benney, D. J. 1966 Long waves on liquid films. *J. Maths & Phys.* **45**, 150–155.

Burelbach, J. P. 1989 Stability of evaporating/condensing liquid films. Ph.D. dissertation, Northwestern University, Evanston, IL.

Davis, S. H. 1976 The stability of time-periodic flows. *Ann. Rev. Fluid Mech.* **8**, 57–74.

Davis, S. H. 1983 Rupture of thin liquid films. In *Waves on Fluid Interfaces* (ed. R. E. Meyer), *Proc. Symp. Math. Res. Center, Univ. of Wisc.* pp. 291–302. Academic.

Davis, S. H. 1987 Thermocapillary instabilities. *Ann. Rev. Fluid Mech.* **19**, 403–435.

Delhaye, J. M. 1974 Jump conditions and entropy sources in two-phase systems. Local instant formulation. *Intl J. Multiphase Flow* **1**, 395–409.

Deryagin, B. V. 1955 *Colloid J. USSR* **17**, 207–214.

Deryagin, B. V. & Kusakov, M. M. 1937 *Izv. Akad. Nauk SSSR, Khim.* **5**, 1119. (1939 *Acta Phys. Chem. USSR* **10**, 25; Deryagin, Kusakov & Lebedeva 1939 *Dokl. Akad. Nauk. SSSR* **23**, 671.)

Dzyaloshinskii, I. E., Lifshitz, E. M. & Pitaevskii, L. P. 1959 *Zh. Eksp. Teor. Fiz.* **37**, 229–241. (Transl. 1960 Van der Waals forces in liquid films. *Sov. Phys. JETP* **10**, 161–170.)

Dzyaloshinskii, I. E. & Pitaevskii, L. P. 1959 *Zh. Eksp. Teor. Fiz.* **36**, 1797–1805. (Transl. 1959 Van der Waals forces in an inhomogeneous dielectric. *Sov. Phys. JETP* **9**, 1282–1287.)

Gumerman, R. J. & Homsy, G. M. 1975 The stability of radially bounded thin films. *Chem. Engng Commun.* **2**, 27–36.

HICKMAN, K. 1952 Studies in high vacuum evaporation. Part III – Surface behaviour in the pot still. *Ind. Engng Chem.* **44**, 1892–1902.

HICKMAN, K. 1972 Torpid phenomena and pump oils. *J. Vac. Sci. Technol.* **9**, 960–976.

HIGUERA, F. J. 1987 The hydrodynamic stability of an evaporating liquid. *Phys. Fluids* **30**, 679–686.

LIFSHITZ, E. M. 1955 *Zh. Eksp. Teor. Fiz.* **29**, 94–110. (Transl. 1956 The theory of molecular attractive forces between solids. *Sov. Phys. JETP* **2**, 73–83.)

MARSCHALL, E. & LEE, C. Y. 1973 Stability of condensate flow down a vertical wall. *Intl J. Heat Mass Transfer* **16**, 41–48.

MILLER, C. A. 1973 Stability of moving surfaces in fluid systems with heat and mass transport. Part II – Combined effects of transport and density difference between phases. *AIChE J.* **19**, 909–915.

OVERBEEK, J. T. G. 1960 Black soap films. *J. Phys. Chem.* **64**, 1178–1183.

PALMER, H. J. 1976 The hydrodynamic stability of rapidly evaporating liquids at reduced pressure. *J. Fluid Mech.* **75**, 487–511.

PALMER, H. J. & MAHESHRI, J. C. 1981 Enhanced interfacial heat transfer by differential vapor recoil instabilities. *Intl J. Heat Mass Transfer* **24**, 117.

PROSPERETTI, A. & PLESSET, M. S. 1984 The stability of an evaporating liquid surface. *Phys. Fluids* **27**, 1590–1602.

RUCKENSTEIN, E. & JAIN, R. K. 1974 Spontaneous rupture of thin liquid films. *J. Chem. Soc. Faraday Trans.* II **70**, 132–147.

SHELUDKO, A. 1967 Thin liquid films. *Adv. Colloid Interface Sci.* **1**, 391–463.

SHEN, S. F. 1961 Some considerations on the laminar stability of time-dependent basic flows. *J. Aerospace Sci.* **28**, 397–404, 417.

SPINDLER, B. 1982 Linear stability of liquid films with interfacial phase change. *Intl J. Heat Mass Transfer* **25**, 161–173.

SPINDLER, B., SOLESIO, J. N. & DELHAYE, J. M. 1978 On the equations describing the instabilities of liquid films with interfacial phase change. *Two-Phase Momentum, Heat and Mass Transfer in Chemical Process and Energy Engineering Systems* (ed. F. Durst, G. V. Tsiklauri & N. H. Afgan), vol. 1, pp. 339–344, Hemisphere.

UNSAL, M. & THOMAS, W. C. 1978 Linearized stability analysis of film condensation. *J. Heat Transfer* **100**, 629–634.

VRIJ, A. 1966 Possible mechanism for the spontaneous rupture of thin, free liquid films. *Discuss. Faraday Soc.* **42**, 23–33.

WILLIAMS, M. B. & DAVIS, S. H. 1982 Nonlinear theory of film rupture. *J. Colloid Interface Sci.* **90**, 220–228.